

Learning functions varying along an active subspace

Hao Liu* Wenjing Liao†

Abstract

Many functions of interest are in a high-dimensional space but exhibit low-dimensional structures. This paper studies regression of a s -Hölder function f in \mathbb{R}^D which varies along an active subspace of dimension d while $d \ll D$. A direct approximation of f in \mathbb{R}^D with an ε accuracy requires the number of samples n in the order of $\varepsilon^{-(2s+D)/s}$. In this paper, we modify the Generalized Contour Regression (GCR) algorithm to estimate the active subspace and use piecewise polynomials for function approximation. GCR is among the best estimators for the active subspace, but its sample complexity is an open question. Our modified GCR improves the efficiency over the original GCR and leads to a mean squared estimation error of $O(n^{-1})$ for the active subspace, when n is sufficiently large. The mean squared regression error of f is proved to be in the order of $(n/\log n)^{-\frac{2s}{2s+d}}$ where the exponent depends on the dimension of the active subspace d instead of the ambient space D . This result demonstrates that GCR is effective in learning low-dimensional active subspaces. The convergence rate is validated through several numerical experiments.

1 Introduction

A vast majority of statistical inference and machine learning problems can be modeled as regression, where the goal is to estimate an unknown function from finite training samples. Nowadays, new challenges are introduced to regression and prediction due to the rise of high-dimensional data in many fields of contemporary science. The well-known curse of dimensionality implies that, in order to achieve a fixed accuracy in prediction, the number of training data must grow exponentially with respect to the dimension of data, which is beyond practical applications.

Fortunately, functions of interest in applications often exhibit low-dimensional structures. In many situations, the response may depend on few variables, or a low-dimensional subspace. For example, in Bioinformatics, the cDNA microarray data have thousands of dimension but an effective classification of tumor types only depends on a subspace of dimension one or two [3]. In engineering, the coefficients of certain elliptic partial differential equations are parameterized by many variables but has a small effective dimension [6]. In photovoltaic industry, there are five input parameters in the single-diode solar cell

*School of Mathematics, Georgia Institute of Technology, 686 Cherry Street, Atlanta, GA 30332 USA (Email: hao.liu@math.gatech.edu).

†School of Mathematics, Georgia Institute of Technology, 686 Cherry Street, Atlanta, GA 30332 USA (Email: wliao60@gatech.edu). This research is supported by NSF DMS 1818751.

model while the maximum power output only depends on a linear combination of these five parameters [7]. Similar low-dimensional models appear in optimization [15], optimal control [41], uncertainty quantification [1], text classification [22] and biomedicine [31, 32].

These applications motivate us to consider the regression model

$$y_i = f(\mathbf{x}_i) + \xi_i = g(\Phi^T \mathbf{x}_i) + \xi_i, \quad (1)$$

where $\mathbf{x} \in \mathbb{R}^D$, $\Phi \in \mathbb{R}^{D \times d}$, $g : \mathbb{R}^d \rightarrow \mathbb{R}$ and $\xi_i \in \mathbb{R}$. The columns of Φ consist of an orthonormal basis of a d -dimensional subspace, i.e., $\Phi^T \Phi = I_d$. The random variable ξ_i models noise, which is independent of the \mathbf{x}_i 's. In this model, the function f is defined on \mathbb{R}^D but only depends on the projection of \mathbf{x} to the subspace spanned by Φ , denoted by \mathcal{S}_Φ . Let \mathcal{S}_Φ be such a space of minimum dimension: $g(\mathbf{v}^T \mathbf{z})$ is not a constant function for any $\mathbf{v} \in \mathcal{S}_\Phi$. Then \mathcal{S}_Φ is called the active subspace (or central subspace) of f . In other words, the function f only varies along the active subspace, and remains the same along any orthogonal direction of the active subspace. This model is also called the single-index model for $d = 1$ and the multi-index model for $d \geq 2$.

The goal of regression is to estimate the function f from n samples of data $\{(\mathbf{x}_i, y_i)\}_{i=1}^n$ where the \mathbf{x}_i 's are independently drawn from a probability measure ρ in \mathbb{R}^D . Given data and the a prior knowledge that f varies along a d -dimensional active subspace, we aim at constructing an empirical estimator $\hat{f} : \mathbb{R}^D \rightarrow \mathbb{R}$ and studying the Mean Squared Error (MSE) $\mathbb{E}_{\{(\mathbf{x}_i, y_i)\}_{i=1}^n} \|\hat{f} - f\|_{L^2(\rho)}^2$.

The central interest of this problem is to estimate the active subspace Φ . A class of methods is based on the gradient $\nabla f(\mathbf{x}) = \Phi \nabla g(\Phi^T \mathbf{x})$. When $d = 1$, ∇f is proportional to the Φ direction, which allows one to estimate Φ from average of the empirical gradients [34, 17, 18]. When $d \geq 2$, the covariance matrix of ∇f is given by $\Phi \int \nabla g(\Phi^T \mathbf{x}) [\nabla g(\Phi^T \mathbf{x})]^T \rho(d\mathbf{x}) \Phi^T$, which gives an estimate of Φ as the eigenspace associated with the top d eigenvalues of this covariance matrix [20, 6]. If the gradient can be accurately estimated, these gradient-based methods lead to a \sqrt{n} -consistent estimation of Φ [18, 6]. In general, the gradient estimation in \mathbb{R}^D requires an exponentially large number of samples in dimension D .

The single-index model while $d = 1$ has been extensively studied in literature. In this case, $g : \mathbb{R} \rightarrow \mathbb{R}$ is called the link function. The minimax mean squared regression error while the link function belongs to the s -Hölder class was proved to be $O(n^{-2s/(2s+1)})$ [13, 24, 4]. These results demonstrate that the optimal algorithm can automatically adapt to the active subspace of dimension 1. For estimation, a lot of methods based on non-convex optimization have been proposed [24, 16, 21, 40] while achieving the global minimum is not guaranteed. It was proved in [16, Chapter 22] that minimizing the empirical risk over the active subspace of dimension 1 and piecewise polynomial approximations to g simultaneously gives rise to the MSE of $O((n/\log n)^{-2s/(2s+1)})$. The main challenge of this approach is to obtain the global minimum due to non-convexity in the optimization. In the context of regression with point queries, an adaptive query algorithm was proposed for the single-index model in [5] with performance guarantees. This algorithm was generalized to the multi-index model in [11]. In the standard regression setting, adaptive queries are not allowed, and samples are given before learning starts.

Estimating the active subspace is called sufficient dimension reduction in statistics. A class of methods related with inverse regression has been developed to estimate the active subspace Φ – see [30, 25] for a comprehensive review. Sliced Inverse Regression (SIR) [28] is the first and most well known estimator. The term “inverse regression”

refers to the conditional expectation $\mathbb{E}(\mathbf{x}|y)$. In SIR, the active subspace is estimated as the eigenspace associated with the top d eigenvalues of $\text{Cov}(\mathbb{E}(\mathbf{x}|y) - \mathbb{E}(\mathbf{x}))$. Similar techniques include kernel inverse regression [42], parametric inverse regression [2] and canonical correlation estimator [12]. These methods are referred as first-order methods since the first-order statistical information was utilized, such as the conditional mean. Their performance crucially depends on the function g and the distribution of data. If g is symmetric about $\mathbf{0}$ along some directions, then those directions can not be recovered by the first-order methods. This issue about symmetry is better addressed by second-order methods which utilize the variance and covariance information of data. Sliced Average Variance Estimation (SAVE) [8] is the first second-order method. Others include contour regression [27], directional regression [26], a hybrid of SIR and SAVE [43], etc. Many of these methods succeed under appropriate assumptions, but these assumptions can be violated when g is not monotonic. For the single-index model, a recent paper [23] proposes a new method called Smallest Vector Regression (SVR), which combines the idea of SIR and SAVE. A performance analysis is provided for the index estimation and regression, while the assumptions are favorable to monotonic g .

This paper focuses on a second-order method called Generalized Contour Regression (GCR) introduced by Li, Zha and Chiaromonte [27]. In comparison with SIR and SAVE mentioned above, GCR does not require g to be monotonic. Empirical experiments suggest that GCR is among the best estimators for the active subspace, but its sample complexity is not well understood yet. In this paper, we consider a modified version of GCR which is more efficient than the original GCR. Our regression scheme consists of the modified GCR for the active subspace estimation and piecewise polynomial approximation of g . Our contributions are

- (i) Our modified GCR improves over the original GCR in efficiency. It gives rise to an mean squared estimation error of $O(n^{-1})$ for the active subspace, when n is sufficiently large.
- (ii) Our regression scheme gives rise to the MSE of f in the order of $(n/\log n)^{-\frac{2s}{2s+d}}$ when n is sufficiently large. This demonstrates that the MSE decays exponentially with an exponent depending on the dimension of the active subspace d , instead of the ambient dimension D .

This paper is organized as follows: We first introduce SCR and GCR in Section 2. Our regression scheme and main results are stated in Section 3. Numerical experiments are provided in Section 4 to validate our theory. Proofs are presented in Section 5, and we conclude in Section 6.

We use lowercase bold letters and capital letters to denote vectors and matrices respectively. $\|\mathbf{x}\|$ is the Euclidean norm of the vector \mathbf{x} and $\|A\|$ is the spectral norm of the matrix A . For two square matrices A and B of the same size, $A \preceq B$ means $B - A$ is positive semi-definite. We use \mathbb{N}_0 to denote nonnegative integers. For a function g , $\text{supp}(g)$ denotes the support of g . For $x \in \mathbb{R}$, $\lfloor x \rfloor$ denotes the largest integer that is no larger than x . Throughout the paper, we use \mathcal{S}_{Φ} and $\mathcal{S}_{\Phi}^{\perp}$ to denote the active subspace and its orthogonal complement, respectively.

2 Active subspace and contour regression

The model in (1) has an ambiguity since the solutions are not unique. The columns of Φ form an orthonormal basis of the active subspace, while the choice of orthonormal basis is not unique. This gives rise to an ambiguity between the basis Φ and the function g , which can be characterized by the following lemma:

Lemma 1. *Consider the model in (1) where the columns of Φ form an orthonormal basis of the active subspace. For any orthogonal matrix $Q \in \mathbb{R}^{d \times d}$, let $\tilde{\Phi} = \Phi Q$ and $\tilde{g}(\mathbf{z}) = g(Q\mathbf{z})$ for any $\mathbf{z} \in \mathbb{R}^d$. Then the columns of $\tilde{\Phi}$ form another orthonormal basis of the active subspace and $g(\Phi^T \mathbf{x}) = \tilde{g}(\tilde{\Phi}^T \mathbf{x})$.*

Lemma 1 shows the representation of f is not unique: if another set of orthonormal basis is picked, the function g changes accordingly. In this paper, we aim to recover one set of orthonormal basis $\hat{\Phi}$ and the corresponding function \hat{g} . The subspace estimation error and regression error are represented by $\|\text{Proj}_{\hat{\Phi}} - \text{Proj}_{\Phi}\|$ and

$$\|\hat{f} - f\|_{L^2(\rho)} := \inf_{\substack{\Phi: \text{an orthonormal basis of } \mathcal{S}_{\Phi} \\ g: \mathbb{R}^d \rightarrow \mathbb{R}, f(\cdot) = g(\Phi^T \cdot)}} \int |\hat{g}(\hat{\Phi}^T \mathbf{x}) - g(\Phi^T \mathbf{x})|^2 \rho(d\mathbf{x}) \quad (2)$$

respectively, which are invariant to the choice of orthonormal basis.

2.1 Simple contour regression

We start with Simple Contour Regression (SCR) [27] which utilizes the fact that the contour directions of f are orthogonal to the active subspace. Let $\alpha > 0$ and define the following conditional covariance matrix:

$$K(\alpha) = \mathbb{E} [(\tilde{\mathbf{x}} - \mathbf{x})(\tilde{\mathbf{x}} - \mathbf{x})^T | |\tilde{y} - y| \leq \alpha],$$

where $(\tilde{\mathbf{x}}, \tilde{y})$ and (\mathbf{x}, y) are two independent samples.

When $d = 1$ and g is a monotonic function, we expect many of the $(\tilde{\mathbf{x}}, \mathbf{x})$ pairs satisfying $|\tilde{y} - y| \leq \alpha$ will have $|\Phi^T \tilde{\mathbf{x}} - \Phi^T \mathbf{x}|$ small while $|\mathbf{w}^T \tilde{\mathbf{x}} - \mathbf{w}^T \mathbf{x}|$ can be arbitrarily large for any $\mathbf{w} \in \mathcal{S}_{\Phi}^{\perp}$. In this case, most of the $\tilde{\mathbf{x}} - \mathbf{x}$ directions satisfying $|\tilde{y} - y| \leq \alpha$ are aligned with $\mathcal{S}_{\Phi}^{\perp}$.

For example, in Figure 1(a), $f(\mathbf{x}) = e^{x_1}$ with $\mathbf{x} = (x_1, x_2) \in [-2, 2] \times [-2, 2]$. This function can be expressed as Model (1) with $\Phi = [1, 0]^T$, $\mathbf{w} = [0, 1]^T$, and $g(z) = e^z$. Consider two inputs $\mathbf{p} = (p_1, p_2)$ and $\tilde{\mathbf{p}} = (\tilde{p}_1, \tilde{p}_2)$ satisfying $|f(\mathbf{p}) - f(\tilde{\mathbf{p}})| \leq \alpha$. Since $e^{-2}|p_1 - \tilde{p}_1| \leq |e^{p_1} - e^{\tilde{p}_1}| = |f(\mathbf{p}) - f(\tilde{\mathbf{p}})|$, the condition $|f(\mathbf{p}) - f(\tilde{\mathbf{p}})| \leq \alpha$ implies $|\Phi^T(\tilde{\mathbf{p}} - \mathbf{p})| = |p_1 - \tilde{p}_1| < e^2 \alpha$. On the other hand, $|\mathbf{w}^T(\tilde{\mathbf{p}} - \mathbf{p})| = |p_2 - \tilde{p}_2| \in [0, 4]$, which is independent of α . In Figure 1(b), 200 samples are uniformly drawn from $[-0.5, 0.5] \times [-0.5, 0.5]$. The $(\mathbf{x}, \tilde{\mathbf{x}})$ pair is connected if $|f(\mathbf{x}) - f(\tilde{\mathbf{x}})| \leq 0.01$. We observe that, almost all connections by SCR in Figure 1(b) are aligned with the \mathbf{w} direction.

SCR estimates the active subspace from the smallest d eigenvectors of $K(\alpha)$. The success of SCR is guaranteed by the following condition:

Condition 1. *There exists $\alpha_c > 0$ such that for any $\alpha \in (0, \alpha_c)$ and unit vectors $\mathbf{v} \in \mathcal{S}_{\Phi}$, $\mathbf{w} \in \mathcal{S}_{\Phi}^{\perp}$, the following holds*

$$\text{var} [\mathbf{w}^T(\tilde{\mathbf{x}} - \mathbf{x}) | |\tilde{y} - y| \leq \alpha] > \text{var} [\mathbf{v}^T(\tilde{\mathbf{x}} - \mathbf{x}) | |\tilde{y} - y| \leq \alpha].$$

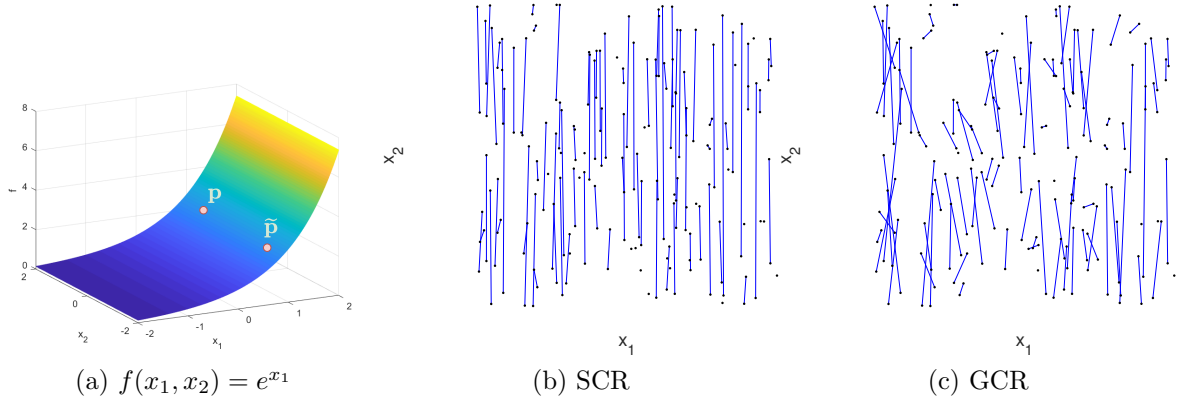


Figure 1: (a) Function $f(x_1, x_2) = e^{x_1}$. When 200 samples are uniformly drawn in $[-0.5, 0.5] \times [-0.5, 0.5]$, (b) and (c) display the connected $(\mathbf{x}, \tilde{\mathbf{x}})$ pairs by SCR (b) and GCR (c), respectively. An $(\mathbf{x}, \tilde{\mathbf{x}})$ pair is connected by SCR in (b) if $|f(\mathbf{x}) - f(\tilde{\mathbf{x}})| \leq 0.01$ and by GCR in (c) if $\hat{V}_y(\mathbf{x}, \tilde{\mathbf{x}}; r) \leq 0.001$ with $r = 0.01$. Here $\hat{V}_y(\mathbf{x}, \tilde{\mathbf{x}}; r)$ is an empirical estimator of $V_f(\mathbf{x}, \tilde{\mathbf{x}})$ to be defined in (5).

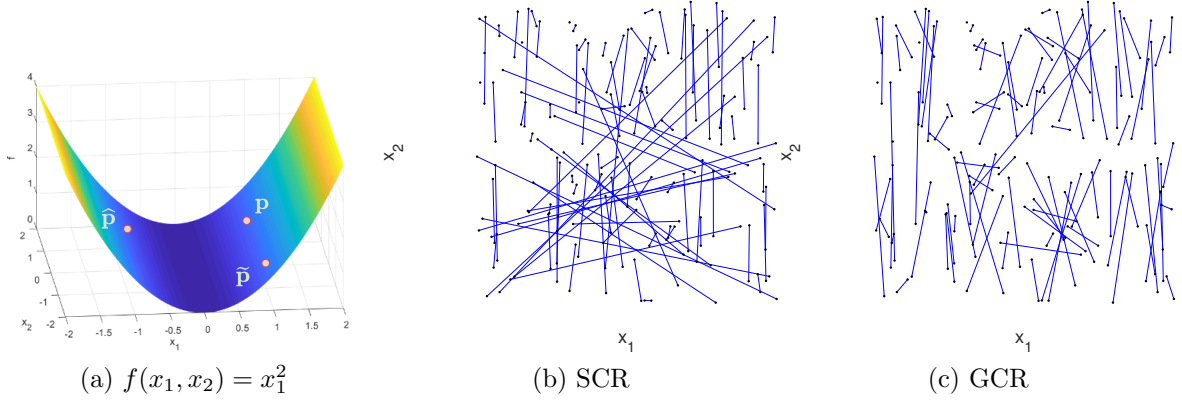


Figure 2: (a) Function $f(x_1, x_2) = x_1^2$. When 200 samples are uniformly drawn in $[-0.5, 0.5] \times [-0.5, 0.5]$, (b) and (c) display the connected $(\mathbf{x}, \tilde{\mathbf{x}})$ pairs by SCR (b) and GCR (c), respectively. An $(\mathbf{x}, \tilde{\mathbf{x}})$ pair is connected by SCR in (b) if $|f(\mathbf{x}) - f(\tilde{\mathbf{x}})| \leq 0.01$ and by GCR in (c) if $\hat{V}_y(\mathbf{x}, \tilde{\mathbf{x}}; r) \leq 0.001$ with $r = 0.01$.

Define the elliptical distribution as

Definition 1 (Elliptical distribution). *Let $\mathbf{x} \in \mathbb{R}^D$ be a random vector with probability distribution ρ . For any unit vector $\mathbf{v} \in \mathbb{R}^D$, we say ρ has an elliptical distribution along the direction \mathbf{v} if $\mathbf{v}^T(\mathbf{x} - \mathbb{E}\mathbf{x})$ and $-\mathbf{v}^T(\mathbf{x} - \mathbb{E}\mathbf{x})$ have the same distribution.*

Condition 1 together with an elliptical distribution of \mathbf{x} along \mathcal{S}_Φ^\perp guarantees that the eigenvectors associated with the smallest d eigenvalues of $K(\alpha)$ span \mathcal{S}_Φ [27].

2.2 Generalized contour regression

Condition 1 does not necessarily hold when $d = 1$ and the function g is not monotonic, as well as when $d > 1$. For example in Figure 2 (a), $f(\mathbf{x}) = x_1^2$ with $\mathbf{x} = (x_1, x_2) \in [-2, 2] \times [-2, 2]$. This function can be expressed in Model (1) with $\Phi = [1, 0]^T$, $\mathbf{w} = [0, 1]^T$

and $g(z) = z^2$. Let $\mathbf{p} = (p_1, p_2)$ and $\hat{\mathbf{p}} = (\hat{p}_1, \hat{p}_2)$ be two inputs satisfying $p_1 > 0, \hat{p}_1 < 0$, and $|f(\mathbf{p}) - f(\hat{\mathbf{p}})| \leq \alpha$ for some small α . Due to symmetry, $|\Phi^T(\hat{\mathbf{p}} - \mathbf{p})| = |\hat{p}_1| + |p_1|$ can be very large, which violates Condition 1. When 200 samples are uniformly drawn in $[-0.5, 0.5] \times [-0.5, 0.5]$, an $(\mathbf{x}, \tilde{\mathbf{x}})$ pair is connected by SCR in Figure 2 (b) if $|f(\mathbf{x}) - f(\tilde{\mathbf{x}})| \leq 0.01$. The ideal connections are along the x_2 direction, but SCR gives many misleading connections since f is not monotonic. When $d > 1$, Condition 1 can be easily violated as well. For any fixed $\mathbf{x} \in \mathbb{R}^D$, the contour $\{\tilde{\mathbf{x}} | f(\tilde{\mathbf{x}}) = f(\mathbf{x})\}$ is a curve or a surface, so $\|\Phi^T(\tilde{\mathbf{x}} - \mathbf{x})\|$ is not necessarily small.

Fortunately, most misleading connections can be identified from a large variance of f along the segment between the two inputs. In Figure 2, $|f(\mathbf{p}) - f(\hat{\mathbf{p}})|$ is small but the variance of f along the segment between \mathbf{p} and $\hat{\mathbf{p}}$ is large. This criterion helps to rule out the misleading connection between \mathbf{p} and $\hat{\mathbf{p}}$.

Replacing the condition of $|y - \tilde{y}| \leq \alpha$ in SCR by a variance condition gives rise to the Generalized Contour Regression (GCR) [27]. Let $\ell(\mathbf{x}_i, \mathbf{x}_j) = \{\mathbf{x} = (1-t)\mathbf{x}_i + t\mathbf{x}_j, t \in [0, 1]\}$ be the segment between \mathbf{x}_i and \mathbf{x}_j . The variance of f along this line is:

$$V_f(\mathbf{x}_i, \mathbf{x}_j) = \text{var}(f(\mathbf{x}) | \mathbf{x} \in \ell(\mathbf{x}_i, \mathbf{x}_j)).$$

In GCR, the covariance matrix is taken to be

$$G(\alpha) = \mathbb{E}[(\tilde{\mathbf{x}} - \mathbf{x})(\tilde{\mathbf{x}} - \mathbf{x})^T | V_f(\tilde{\mathbf{x}}, \mathbf{x}) \leq \alpha], \quad (3)$$

where $\alpha > 0$ is a fixed number. One can expect the following assumption based on the model in (1).

Assumption 1. *There exist $\alpha_{\text{thresh}} > 0$, $C_0 > 0$ and a function $\phi : \mathbb{R} \rightarrow \mathbb{R}$ satisfying $\phi(\alpha) < C_0$ for $\alpha \in (0, \alpha_{\text{thresh}})$, such that: for any $\alpha \in (0, \alpha_{\text{thresh}})$ and unit vectors $\mathbf{v} \in \mathcal{S}_\Phi$, $\mathbf{w} \in \mathcal{S}_\Phi^\perp$, the followings hold*

$$\begin{aligned} \text{var}[\mathbf{v}^T(\tilde{\mathbf{x}} - \mathbf{x}) | V_f(\tilde{\mathbf{x}}, \mathbf{x}) \leq \alpha] &\leq \phi(\alpha), \\ \text{var}[\mathbf{w}^T(\tilde{\mathbf{x}} - \mathbf{x}) | V_f(\tilde{\mathbf{x}}, \mathbf{x}) \leq \alpha] &\geq C_0. \end{aligned}$$

Assumption 1 is natural for the model in (1). It is shown in [27, Theorem 4.2] that under the model in (1), one always has

$$\text{var}[\mathbf{v}^T(\tilde{\mathbf{x}} - \mathbf{x}) | V_f(\tilde{\mathbf{x}}, \mathbf{x}) \leq \alpha] < \text{var}[\mathbf{w}^T(\tilde{\mathbf{x}} - \mathbf{x}) | V_f(\tilde{\mathbf{x}}, \mathbf{x}) \leq \alpha]$$

when α is sufficiently small.

An $(\mathbf{x}, \tilde{\mathbf{x}})$ pair is said to be connected if $V_f(\mathbf{x}, \tilde{\mathbf{x}}) \leq \alpha$. In Figure 2, even though $|f(\mathbf{p}) - f(\hat{\mathbf{p}})|$ is small, the variance $V_f(\mathbf{p}, \hat{\mathbf{p}})$ is large. When α is small, the condition of $V_f(\mathbf{p}, \hat{\mathbf{p}}) \leq \alpha$ is violated so the $(\mathbf{p}, \hat{\mathbf{p}})$ pair is not connected. We expect all connected pairs by GCR to be aligned with the x_2 direction, such as $(\mathbf{p}, \tilde{\mathbf{p}})$. For such connected pairs, it is very likely that $p_1 \tilde{p}_1 > 0$, which implies $|\Phi^T(\tilde{\mathbf{p}} - \mathbf{p})| = |\tilde{p}_1 - p_1| \leq \alpha / \min(p_1, \tilde{p}_1)$ while $|\mathbf{w}^T(\tilde{\mathbf{p}} - \mathbf{p})| = |\tilde{p}_2 - p_2| \in [0, 4]$ is independent of α . When 200 samples are uniformly drawn in $[-0.5, 0.5] \times [-0.5, 0.5]$, an $(\mathbf{x}, \tilde{\mathbf{x}})$ pair is connected by GCR in Figure 2(c) if an empirical estimator of $V_f(\mathbf{x}, \tilde{\mathbf{x}})$ (see (5)) is no more than 0.001. We observe that, most connections by GCR are along the x_2 direction, and many misleading connections by SCR are ruled out.

Assumption 1 together with an elliptical distribution imply that, when $\alpha < \alpha_{\text{thresh}}$ the eigenspace of $G(\alpha)$ associated with the smallest d eigenvalues is \mathcal{S}_Φ and the rest of the eigenvectors will span \mathcal{S}_Φ^\perp .

Proposition 1. Assume ρ has an elliptical distribution along any direction $\mathbf{w} \in \mathcal{S}_\Phi^\perp$. Let $\lambda_1 \geq \lambda_2 \geq \dots \geq \lambda_D$ be the eigenvalues of $G(\alpha)$. Under Assumption 1, the followings hold for any $\alpha \in (0, \alpha_{\text{thresh}})$:

- $\lambda_j \geq C_0$ for $j = 1, \dots, D - d$ and $\lambda_k \leq \phi(\alpha)$ for $k = D - d + 1, \dots, D$.
- The eigenvectors of $G(\alpha)$ associated with $\{\lambda_j\}_{j=1}^{D-d}$ span \mathcal{S}_Φ^\perp and the eigenvectors associated with $\{\lambda_k\}_{k=D-d+1}^D$ span \mathcal{S}_Φ .

Proposition 1 was first proved in [27] and we include its proof in Supplementary materials A for completeness. In practice, the segment $\ell(\mathbf{x}_i, \mathbf{x}_j)$ has 0 measure, so it is unlikely to have data lying exactly on $\ell(\mathbf{x}_i, \mathbf{x}_j)$. We approximate $V_f(\mathbf{x}_i, \mathbf{x}_j)$ by the variance of y in a narrow tube enclosing $\ell(\mathbf{x}_i, \mathbf{x}_j)$ with radius r (see Figure 3). Let $d(\mathbf{x}, \ell(\mathbf{x}_i, \mathbf{x}_j))$ be the distance from \mathbf{x} to $\ell(\mathbf{x}_i, \mathbf{x}_j)$: $d(\mathbf{x}, \ell(\mathbf{x}_i, \mathbf{x}_j)) = \inf_{\mathbf{z} \in \ell(\mathbf{x}_i, \mathbf{x}_j)} \|\mathbf{x} - \mathbf{z}\|$. We define $T_{ij}(r)$ as the tube enclosing $\ell(\mathbf{x}_i, \mathbf{x}_j)$ with radius r as follows

$$T_{ij}(r) \triangleq \{\mathbf{x} | d(\mathbf{x}, \ell(\mathbf{x}_i, \mathbf{x}_j)) \leq r, (\mathbf{x} - \mathbf{x}_i) \cdot (\mathbf{x}_j - \mathbf{x}_i) \geq 0, (\mathbf{x} - \mathbf{x}_j) \cdot (\mathbf{x}_i - \mathbf{x}_j) \geq 0\}.$$

The variance of y in $T_{ij}(r)$ is

$$V_y(\mathbf{x}_i, \mathbf{x}_j, r) = \text{var}(y | \mathbf{x} \in T_{ij}(r)). \quad (4)$$

The empirical counterpart of $V_y(\mathbf{x}_i, \mathbf{x}_j, r)$ based on the data $\{(\mathbf{x}_i, y_i)\}_{i=1}^n$ is

$$\hat{V}_y(\mathbf{x}_i, \mathbf{x}_j, r) = \frac{1}{\hat{n}_{ij}(r) - 1} \sum_{\mathbf{x}_k \in T_{ij}(r)} (y_k - \bar{y}_{ij})^2, \text{ where } \bar{y}_{ij} = \frac{1}{\hat{n}_{ij}(r)} \sum_{\mathbf{x}_k \in T_{ij}(r)} y_k, \quad (5)$$

and $\hat{n}_{ij}(r) = \#\{\mathbf{x}_k \in T_{ij}(r)\}$.

We next define the empirical covariance matrix associated with (3). Fix $\alpha > 0$ and $r > 0$. Among the matrices $(\mathbf{x}_i - \mathbf{x}_j)(\mathbf{x}_i - \mathbf{x}_j)^T$ satisfying $\hat{V}_y(\mathbf{x}_i, \mathbf{x}_j, r) \leq \alpha$, many of them are dependent. It is sufficient to take the empirical covariance matrix as the sum of independent ones. Let $\mathcal{A} \in \{0, 1\}^{n \times n}$ be a matrix with entries in $\{0, 1\}$ such that all (i, j) indices with $\mathcal{A}(i, j) = 1$ satisfy $\hat{V}_y(\mathbf{x}_i, \mathbf{x}_j, r) \leq \alpha$ and the matrices $\{(\mathbf{x}_i - \mathbf{x}_j)(\mathbf{x}_i - \mathbf{x}_j)^T : \mathcal{A}(i, j) = 1\}$ are independent. The empirical covariance of (3) is

$$\hat{G}(\alpha, r) = \frac{1}{\hat{n}_\alpha} \sum_{(i,j): \mathcal{A}(\mathbf{x}_i, \mathbf{x}_j)=1} (\mathbf{x}_i - \mathbf{x}_j)(\mathbf{x}_i - \mathbf{x}_j)^T \quad (6)$$

where $\hat{n}_\alpha = \#\{(i, j) : \mathcal{A}(\mathbf{x}_i, \mathbf{x}_j) = 1\}$. Given a data set, the matrix \mathcal{A} is not unique. In this paper, we use the matrix \mathcal{A} given by Algorithm 1. Algorithm 1 is more efficient than the original GCR in the sense that it outputs at most $n/2$ connected pairs while the original GCR may use $O(n^2)$ connected pairs. In the original GCR, $\hat{V}_y(\mathbf{x}_i, \mathbf{x}_j, r)$ is computed for every $(\mathbf{x}_i, \mathbf{x}_j)$ pair. In Algorithm 1, once a point is connected, we remove it from the rest of the computation, so the computational cost is greatly reduced. Moreover, our theory and numerical experiments show that the convergence rate is not affected.

Although the ideas behind GCR are natural, the estimation error of GCR has never been analyzed due to its complexity. This paper is devoted to an error analysis of GCR.

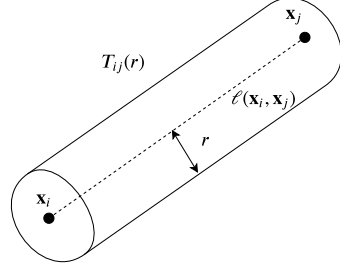


Figure 3: $T_{ij}(r)$: the tube enclosing $\ell(\mathbf{x}_i, \mathbf{x}_j)$ with radius r .

Algorithm 1: Construction of $\widehat{G}(\alpha, r)$ in GCR

Input: $\mathcal{S} = \{(\mathbf{x}_i, y_i)\}_{i=1}^n$ and $\alpha > 0, r > 0$.
Initialization: $\widehat{G} = 0, \widehat{n}_\alpha = 0$ and $\mathcal{A} = \mathbf{0}_{n \times n}$.
while $\#\mathcal{S} > 1$ **do**
 Index data in \mathcal{S} as $\{(\mathbf{x}_{i_k}, y_{i_k})\}, k = 1, \dots, \#\mathcal{S}$.
 for $k = 2$ **to** $\#\mathcal{S}$ **do**
 if $\widehat{V}_y(\mathbf{x}_{i_1}, \mathbf{x}_{i_k}, r) \leq \alpha$ **then**
 $\widehat{G} = \widehat{G} + (\mathbf{x}_{i_1} - \mathbf{x}_{i_k})(\mathbf{x}_{i_1} - \mathbf{x}_{i_k})^T$,
 $\mathcal{A}(i_1, i_k) = 1$,
 $\widehat{n}_\alpha = \widehat{n}_\alpha + 1$,
 $\mathcal{S} = \mathcal{S} \setminus \{\mathbf{x}_{i_1}, \mathbf{x}_{i_k}\}$
 break
 end
 end
 $\mathcal{S} = \mathcal{S} \setminus \{\mathbf{x}_{i_1}\}$
end
 $\widehat{G}(\alpha, r) = \widehat{G} / \widehat{n}_\alpha$.

3 Main Results

3.1 Assumptions

In order to guarantee the success of GCR, we introduce the following assumptions on ρ , requiring that i) ρ is supported on a bounded domain; ii) the measure of every tube is sufficiently large; iii) ρ has an elliptical distribution along any direction in \mathcal{S}_Φ^\perp .

Assumption 2. *Suppose the probability measure ρ satisfies the following assumptions:*

- i) **[Boundedness]** $\text{supp}(\rho)$ is bounded by $B > 0$: for every \mathbf{x} sampled from ρ , $\|\mathbf{x}\| \leq B$ almost surely.
- ii) **[Measure of tube]** There exists $c_0 > 0$ such that, for any $\mathbf{x}_i, \mathbf{x}_j \in \text{supp}(\rho)$ and any $r \in (0, \|\mathbf{x}_i - \mathbf{x}_j\|/4)$,

$$\rho(T_{ij}(r)) \geq c_0 r^{D-1} \|\mathbf{x}_i - \mathbf{x}_j\|. \quad (7)$$

- iii) **[Elliptic distribution]** ρ has an elliptical distribution along any direction $\mathbf{w} \in \mathcal{S}_\Phi^\perp$.

Assumption 2(ii) guarantees sufficient amount of points in every tube so that $V_y(\mathbf{x}_i, \mathbf{x}_j, r)$ in (4) can be well approximated by its empirical quantity $\widehat{V}_y(\mathbf{x}_i, \mathbf{x}_j, r)$ in (5). Assumption 2(ii) is satisfied if ρ has a density bounded away from 0. Assumption 2(iii) is common in inverse regression, but GCR is more robust against nonellipticity than SIR and SCR (see Example 1 in Section 4).

Definition 2 (Lipschitz functions). *A function g is Lipschitz with Lipschitz constant L_g if*

$$|g(\mathbf{z}) - g(\widetilde{\mathbf{z}})| \leq L_g \|\mathbf{z} - \widetilde{\mathbf{z}}\|, \quad \forall \mathbf{z}, \widetilde{\mathbf{z}} \in \text{supp}(g).$$

Algorithm 2: Regression of f

Input: $\{(\mathbf{x}_i, y_i)\}_{i=1}^{2n}$, parameters α, r, s and dimension d .

Step 1: Split data to two subsets $\mathcal{S}_1 = \{(\mathbf{x}_i, y_i)\}_{i=1}^n$ and $\mathcal{S}_2 = \{(\mathbf{x}_i, y_i)\}_{i=n+1}^{2n}$.

Step 2 (GCR): Compute the covariance matrix $\widehat{G}(\alpha, r)$ using \mathcal{S}_1 according to Algorithm 1.

$\widehat{\Phi} \leftarrow$ eigenvectors associated with the smallest d eigenvalues of $\widehat{G}(\alpha, r)$.

Step 3 (Regression): Compute \widehat{g} as the piecewise polynomial of degree k to fit the data $\{(\widehat{\Phi}^T \mathbf{x}_i, y_i)\}_{i=n+1}^{2n}$, according to (15), where $k = \lfloor s + 1 \rfloor - 1$.

Output: Recovered subspace $\widehat{\Phi}$ and function \widehat{g} such that $\widehat{f}(\mathbf{x}) = \widehat{g}(\widehat{\Phi}^T \mathbf{x})$.

Definition 3 (Hölder functions). *Let $s = k + \beta$ for some $k \in \mathbb{N}_0$ and $0 < \beta \leq 1$, and $C_g > 0$. A function $g : \mathbb{R}^d \rightarrow \mathbb{R}$ is called (s, C_g) -smooth if for every $\boldsymbol{\alpha} = (\alpha_1, \dots, \alpha_d), \alpha_i \in \mathbb{N}_0, |\boldsymbol{\alpha}| \leq k$, the partial derivative $D^{\boldsymbol{\alpha}}g := \frac{\partial^k g}{\partial x_1^{\alpha_1} \dots \partial x_d^{\alpha_d}}$ exists and satisfies*

$$\begin{aligned} \sup_{|\boldsymbol{\alpha}| < k} \sup_{\mathbf{z}} |D^{\boldsymbol{\alpha}}g(\mathbf{z})| &< +\infty, \\ |D^{\boldsymbol{\alpha}}g(\mathbf{z}) - D^{\boldsymbol{\alpha}}g(\widetilde{\mathbf{z}})| &\leq C_g \|\mathbf{z} - \widetilde{\mathbf{z}}\|^\beta, \quad \forall \mathbf{z}, \widetilde{\mathbf{z}} \in \text{supp}(g), |\boldsymbol{\alpha}| = k, \end{aligned}$$

where $|\boldsymbol{\alpha}| = \sum_{j=1}^d \alpha_j$.

In this paper, the function g is assumed to be (s, C_g) smooth.

Assumption 3. *The function $g : \mathbb{R}^d \rightarrow \mathbb{R}$ is (s, C_g) -smooth with $s \geq 1$.*

Assumption 2 and 3 imply the followings:

- i) g is Lipschitz as $s \geq 1$. We use L_g to denote its Lipschitz constant.
- ii) g is bounded by Assumption 2 (i) and the Lipschitz property above. We use M to denote its bound such that $|g| \leq M \leq |g(\mathbf{0})| + L_g B$.

Assumption 4. *The noise ξ has zero mean and is bounded: $\mathbb{E}\xi = 0$ and $\xi \in [-\sigma, \sigma]$ almost surely.*

3.2 Regression scheme

Given $2n$ samples denoted by $\mathcal{S} = \{(\mathbf{x}_i, y_i)\}_{i=1}^{2n}$, we evenly split the data into two subsets $\mathcal{S}_1 = \{(\mathbf{x}_i, y_i)\}_{i=1}^n$ and $\mathcal{S}_2 = \{(\mathbf{x}_i, y_i)\}_{i=n+1}^{2n}$, while \mathcal{S}_1 and \mathcal{S}_2 are used to estimate the active subspace and the function g , respectively. Our regression scheme is summarized in Algorithm 2.

The active subspace is estimated from the eigenvectors associated with the smallest d eigenvalues of $\widehat{G}(\alpha, r)$. In GCR, α and r are two important parameters which need to be properly chosen. Let $\nu > 0$ be a fixed constant, and denote

$$\alpha_0 = \max \left\{ C_2 \left(\frac{\log n}{n} \right)^{\frac{1}{\bar{D}}}, C_3 \left(\frac{\log n}{n} \right)^{\frac{1}{\bar{D}+2}} \right\} \quad (8)$$

with $C_1 = (4L_g^2 \max(5B, 2))^{-1}$, $C_2 = \left(\frac{56\nu L_g^2}{3c_0 C_1^{D-1}}\right)^{\frac{1}{D}}$, $C_3 = \left(\frac{256\nu(M+\sigma)^4 L_g^2}{c_0 C_1^{D-1}}\right)^{\frac{1}{D+2}}$, where the parameters L_g, B, c_0, σ, M are defined in Assumption 2-4. We set

$$\alpha = 4dL_g^2 B^2 \left(\frac{\log n}{n}\right)^{\frac{1}{D}} + \alpha_0 + 3\sigma^2 \text{ and } r = C_1 \alpha_0. \quad (9)$$

After the active subspace is estimated as $\widehat{\Phi} \in \mathbb{R}^{D \times d}$, the next step is to estimate the function g from the data $\{(\mathbf{z}_i, y_i)\}_{i=n+1}^{2n}$, where $\mathbf{z}_i = \widehat{\Phi}^T \mathbf{x}_i \in \mathbb{R}^d$. A rich class of nonparametric regression techniques [16, 37, 38] can be used to estimate g , such as kNN, kernel regression, polynomial partitioning estimates, etc. In this paper, we will present the results of polynomial partitioning estimates.

The data $\{(\mathbf{z}_i, y_i)\}_{i=n+1}^{2n}$ satisfies the following model

$$y_i = g(\mathbf{z}_i) + \tilde{\xi}_i, \quad i = n+1, \dots, 2n \quad (10)$$

with noise $\tilde{\xi}_i$ given by

$$\tilde{\xi}_i = y_i - g(\widehat{\Phi}^T \mathbf{x}_i) = g(\Phi^T \mathbf{x}_i) - g(\widehat{\Phi}^T \mathbf{x}_i) + \xi_i. \quad (11)$$

Due to the mismatch between $\widehat{\Phi}$ and Φ , the noise $\tilde{\xi}_i$ has a bias and its conditional mean at $\mathbf{z} = \widehat{\Phi}^T \mathbf{x}$ is

$$\eta(\mathbf{z}) := \mathbb{E}[\tilde{\xi} | \widehat{\Phi}^T \mathbf{x} = \mathbf{z}] = \mathbb{E}[g(\Phi^T \mathbf{x}) - g(\widehat{\Phi}^T \mathbf{x}) | \widehat{\Phi}^T \mathbf{x} = \mathbf{z}], \quad (12)$$

where the expectation is taken over $\mathbf{x} \sim \rho$ and ξ , conditioning on $\widehat{\Phi}^T \mathbf{x} = \mathbf{z}$. This function is bounded such that $\|\eta\|_\infty \leq L_g B \|\widehat{\Phi} - \Phi\|$. We use

$$b_{\text{bias}}^2 = L_g^2 B^2 \|\widehat{\Phi} - \Phi\|^2 \quad (13)$$

to denote an upper bound of the squared bias in noise.

The measure ρ is bounded by Assumption 2(i), which implies $\mathbf{z}_i \in [-B, B]^d$. For a fixed positive integer K , let \mathcal{F}_k be the space of piecewise polynomials of degree no more than k on the partition of $[-B, B]^d$ into K^d cubes with side length $2B/K$. If g is (s, C_g) smooth, the polynomial degree k should be chosen as $k = \lfloor s + 1 \rfloor - 1$. Consider the piecewise polynomial estimator of order k :

$$\tilde{g}(\mathbf{z}) = \arg \min_{h \in \mathcal{F}_k} \frac{1}{n} \sum_{i=n+1}^{2n} |h(\mathbf{z}_i) - y_i|^2. \quad (14)$$

The minimizer \tilde{g} may take arbitrary value while g is bounded by M . The final estimator \widehat{g} is truncated such that

$$\widehat{g}(\mathbf{z}) = T_M \tilde{g}(\mathbf{z}) = \begin{cases} \tilde{g}(\mathbf{z}), & \text{if } |\tilde{g}(\mathbf{z})| \leq M, \\ M \cdot \text{sign}(\tilde{g}(\mathbf{z})), & \text{otherwise.} \end{cases} \quad (15)$$

The parameter K determines the size of the partition, which we set as

$$K = \left\lceil \frac{n}{\max(\sigma^2 + 2C_8 n^{-1}, 2M^2 + 4C_8 n^{-1}) \log n} \right\rceil^{\frac{1}{2s+d}} \quad (16)$$

with the constants

$$\begin{aligned} C_4 &= (C_0 - \phi(\alpha + \alpha_0 + 3\sigma^2))^2, \quad C_5 = 1152B^4, \quad C_6 = 64B^2(C_0 - \phi(\alpha + \alpha_0 + 3\sigma^2)), \\ C_7 &= \frac{C_5}{C_4}(\log(2D) + 2D + 1) + 8 + \frac{8DC_6^2}{C_4^2}, \\ C_8 &= dC_7L_g^2B^2. \end{aligned} \quad (17)$$

The goal of this paper is to give an error analysis of \hat{f} . The Mean Squared Error (MSE) of \hat{f} is defined as

$$\mathbb{E}\|\hat{f}(\mathbf{x}) - f(\mathbf{x})\|_{L^2(\rho)}^2 = \mathbb{E}_{\{(\mathbf{x}_i, y_i)\}_{i=1}^{2n}} \int |\hat{f}(\mathbf{x}) - f(\mathbf{x})|^2 \rho(d\mathbf{x}),$$

where the expectation is taken over the samples $\{(\mathbf{x}_i, y_i)\}_{i=1}^{2n}$. For any $\mathbf{x} \in \mathbb{R}^D$,

$$\begin{aligned} |\hat{f}(\mathbf{x}) - f(\mathbf{x})|^2 &= |\hat{g}(\hat{\Phi}^T \mathbf{x}) - g(\Phi^T \mathbf{x})|^2 \\ &\leq 2|g(\hat{\Phi}^T \mathbf{x}) - g(\Phi^T \mathbf{x})|^2 + 2|\hat{g}(\hat{\Phi}^T \mathbf{x}) - g(\hat{\Phi}^T \mathbf{x})|^2 \\ &\leq 2L_g^2\|\hat{\Phi} - \Phi\|^2\|\mathbf{x}\|^2 + 2|\hat{g}(\hat{\Phi}^T \mathbf{x}) - g(\hat{\Phi}^T \mathbf{x})|^2. \end{aligned} \quad (18)$$

The first term captures the estimation error of the active subspace by GCR, and the second terms captures the regression error of g .

Notice that the active subspace has infinitely many sets of orthonormal basis, which gives non-unique representations of f . Since the regression error in (2) is taken for the infimum over all possible representations of f , we can refer to the columns of Φ and $\hat{\Phi}$ as the canonical vectors. Let $\frac{\pi}{2} \geq \theta_1 \geq \theta_2 \geq \dots \geq \theta_d \geq 0$ be the canonical angles between the subspace spanned by Φ and $\hat{\Phi}$. Specifically, we let $\hat{\Phi} = [\hat{\phi}_1 \ \hat{\phi}_2 \ \dots \ \hat{\phi}_d]$ and $\Phi = [\phi_1 \ \phi_2 \ \dots \ \phi_d]$ such that $\cos \theta_k = \phi_k^T \hat{\phi}_k$ for $k = 1, \dots, d$. According to [35, Theorem 5.5], the largest canonical angle is related with orthogonal projections such that $\sin \theta_1 = \|\text{Proj}_{\hat{\Phi}} - \text{Proj}_{\Phi}\|$, which implies

$$\|\hat{\Phi} - \Phi\|^2 \leq 2d\|\text{Proj}_{\hat{\Phi}} - \text{Proj}_{\Phi}\|^2, \quad (19)$$

to be proved in Supplementary materials G.

3.3 Active subspace error

Our central interest is to estimate the active subspace. The quality of this estimation is measured by $\|\text{Proj}_{\hat{\Phi}} - \text{Proj}_{\Phi}\|$. Our first result in Theorem 1 shows that $\|\text{Proj}_{\hat{\Phi}} - \text{Proj}_{\Phi}\|^2 = O(n^{-1})$ under Assumption 1-4 (see its proof in Section 5.1).

Theorem 1. *Let $\{\mathbf{x}_i\}_{i=1}^n$ be i.i.d. samples of a probability measure ρ and $\{y_i\}_{i=1}^n$ follows the model in (1), under Assumption 1-4. For a fixed $\nu > 2$, set α and r according to (9). If n is sufficiently large and σ is sufficiently small such that*

$$\alpha + \alpha_0 + 3\sigma^2 < \alpha_{\text{thresh}}, \quad (20)$$

then for any $t \in (0, 2)$,

$$\mathbb{P}\{\|\text{Proj}_{\hat{\Phi}} - \text{Proj}_{\Phi}\| \geq t\} \leq 2D \exp\left(\frac{-(C_0 - \phi(\alpha + \alpha_0 + 3\sigma^2))^2 nt^2}{64B^2(18B^2 + (C_0 - \phi(\alpha + \alpha_0 + 3\sigma^2))t)}\right) + 4n^{-(\nu-2)}. \quad (21)$$

Integrating the probability in (21) gives rise to the following mean squared error for the active subspace (see its proof in Section 5.2):

Corollary 1. *Under the conditions in Theorem 1, setting $\nu \geq 3$ gives rise to*

$$\mathbb{E}\|\text{Proj}_{\hat{\Phi}} - \text{Proj}_{\Phi}\|^2 \leq \frac{C_7}{n} \quad (22)$$

where C_7 is defined in (17).

Corollary 1 implies that the mean squared error for the active subspace estimation converges in the rate of $O(n^{-1})$, when the sample size is sufficiently large and noise is sufficiently small such that (20) is satisfied. This condition results from an accurate estimation of the variance $V_f(\mathbf{x}_i, \mathbf{x}_j)$, which requires sufficiently amount of points in the tube $T_{ij}(r)$. Theorem 1 and Corollary 1 guarantee a fast convergence rate independent of the dimension D .

3.4 Regression error

After the active subspace is estimated as $\hat{\Phi}$, the function g can be estimated according to (14) and (15). The following theorem provides an error bound of $\mathbb{E}\|\hat{f}(\mathbf{x}) - f(\mathbf{x})\|_{L^2(\rho)}^2$ (see its proof in Section 5.3).

Theorem 2. *Let $\{\mathbf{x}_i\}_{i=1}^{2n}$ be i.i.d. samples of a probability measure ρ and $\{y_i\}_{i=1}^{2n}$ be sampled according to the model in (1), under Assumption 1-4. Set α, r according to (9) with $\nu \geq 3$ and set K according to (16). Let \hat{f} be the output of Algorithm 2. If n is sufficiently large and σ is sufficiently small such that (20) is satisfied, then*

$$\mathbb{E}\|\hat{f}(\mathbf{x}) - f(\mathbf{x})\|_{L^2(\rho)}^2 \leq \frac{16C_8}{n} + 2C \left(\frac{\max(\sigma^2 + 2C_8n^{-1}, 2M^2 + 4C_8n^{-1}) \log n}{n} \right)^{\frac{2s}{2s+d}}. \quad (23)$$

where $C > 0$ is a constant depending on d, k, s, C_g, B, M , and C_8 are defined in (17).

Theorem 2 demonstrates that if GCR is used to estimate the active subspace, the mean squared regression error decays exponentially in n with an exponent depending on d , instead of D . GCR can effectively exploits the low-dimension structure of the function and gives a faster rate of convergence in comparison with a direct regression in \mathbb{R}^D .

4 Numerical experiments

In this section, we provide numerical experiments to demonstrate the performance of the modified GCR in Algorithm 1 and the regression scheme in Algorithm 2. The data $\{(\mathbf{x}_i, y_i)\}_{i=1}^n$ are sampled according to the model in (1) with $\xi_i \sim N(0, \sigma^2)$. The noise is $p\%$ if $\sigma = p\% \sqrt{1/n \sum_{i=1}^n f^2(\mathbf{x}_i)}$. In all experiments, 90% of the given data is used for training and 10% is used for testing. Training data are used for active subspace estimation by GCR, SCR or SIR respectively and regression of g is performed by Gaussian kernel regression through the MATLAB built-in function `fitrkernl`. Test data are used to compute the active subspace estimation error $\|\text{Proj}_{\hat{\Phi}} - \text{Proj}_{\Phi}\|_2$ and the regression error

$$\text{Regression error}^2 = \frac{1}{n_{\text{test}}} \sum_{(\mathbf{x}_i, y_i) \in \text{test set}} (\hat{f}(\mathbf{x}_i) - y_i)^2$$

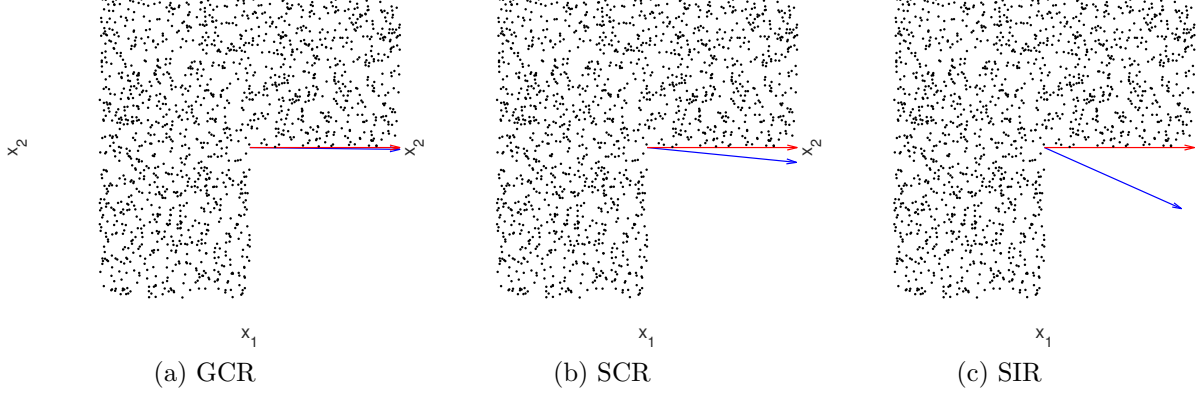


Figure 4: (Example 1) Active subspace estimation by GCR, SCR and SIR when \mathbf{x} is not elliptically distributed. Samples are displayed in black dots and the direction of Φ is represented by a red arrow. The direction of $\hat{\Phi}$ is shown in a blue arrow in (a) by GCR, (b) by SCR and (c) by SIR. We observe that GCR is more robust than SCR and SIR when \mathbf{x} is not elliptically distributed.

where n_{test} is the number of test data. In GCR, the parameter r is chosen in the order of $n^{-1/D}$. We set $r = 2n^{-1/D}$ without specification.

We expect $\mathbb{E}\|\text{Proj}_{\hat{\Phi}} - \text{Proj}_{\Phi}\|_2 \sim n^{-1/2}$, so $\log_{10} \|\text{Proj}_{\hat{\Phi}} - \text{Proj}_{\Phi}\|_2$ scales linearly with respect to $\log_{10} n$, with a slope of $-1/2$, independently of d and D .

4.1 Example 1

In the first example, we investigate the sensitivity of GCR, SCR and SIR to the condition of elliptical distributions in Assumption 2(iii). Let $f(\mathbf{x}) = x_1^2$ where $\mathbf{x} = (x_1, x_2)^T \in \mathbb{R}^2$. This function can be expressed as the model in (1) with $\Phi = [1, 0]^T$ and $g(z) = z^2$ where $z = \Phi^T \mathbf{x}$. We sample \mathbf{x} uniformly in the domain $[-0.5, 0.5] \times [-0.5, 0.5]$ excluding the forth quarter, which violates the condition of elliptical distributions. We set $r = 0.01$, $\alpha = 0.001$ in GCR, $\alpha = 0.01$ in SCR and 10 slices in SIR. Figure 4 shows 1500 samples of \mathbf{x} (black dots), the direction of Φ (red arrow) and the direction of $\hat{\Phi}$ (blue arrow). We observe that GCR is more robust than SCR and SIR when \mathbf{x} is not elliptically distributed.

4.2 Example 2

In the second example, we test and compare the performance of GCR, SCR and SIR on two monotonic single index models:

$$f_1(\mathbf{x}) = \left(\frac{x_1 + x_2}{2} \right)^3, \quad f_2(\mathbf{x}) = e^{(x_1 + x_2)/2}, \quad \mathbf{x} \in \mathbb{R}^{10}.$$

Both functions can be expressed in model (1) with $D = 10$ and $d = 1$. They are $f_1(\mathbf{x}) = g_1(z) = (z/\sqrt{2})^3$ and $f_2(\mathbf{x}) = g_2(z) = e^{z/\sqrt{2}}$ with $z = \Phi^T \mathbf{x}$ where $\Phi = \frac{1}{\sqrt{2}}(\mathbf{e}_1 + \mathbf{e}_2)$. Here $\mathbf{e}_i \in \mathbb{R}^D$ has 1 in the i th entry and 0 everywhere else. In this and the following examples, the \mathbf{x}_i 's are uniformly sampled from $[-1, 1]^D$, and the sample size varies such that $n = 10^3, 10^{3.3}, 10^{3.6}, 10^{3.9}, 10^{4.2}, 10^{4.5}$.

We compare GCR, SCR and SIR with 5% noise. Figure 5 shows the log-log plot of the active subspace estimation error versus n for each function. In GCR, we use $\alpha = n^{-D}/200$

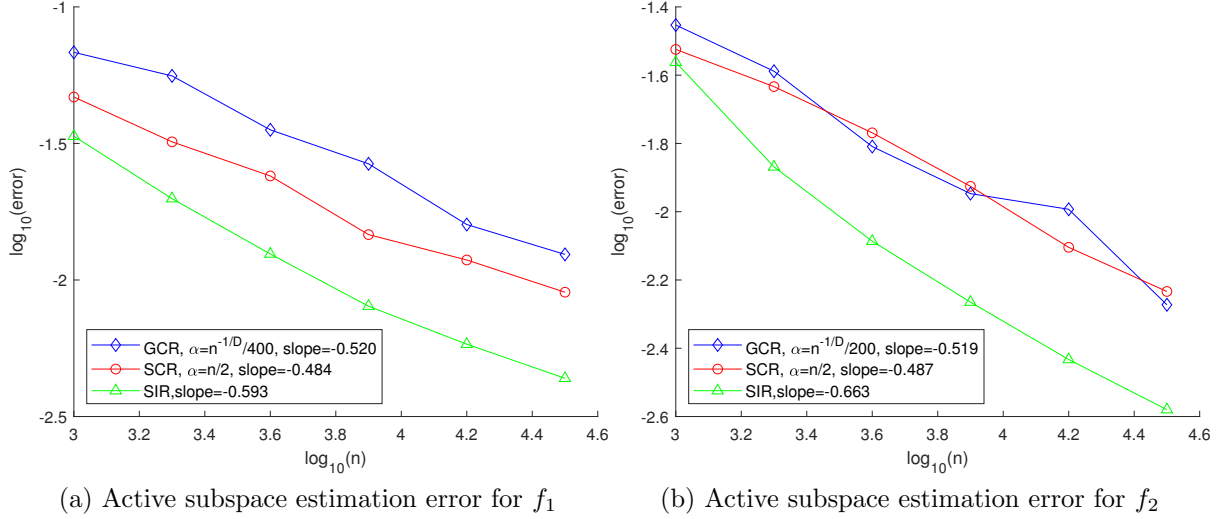


Figure 5: (Example 2 – comparison of GCR, SCR and SIR with 5% noise.) Log-log plot of the active subspace estimation error versus n for f_1 (a) and f_2 (b). SIR has the best performance when the function g is monotonic.

for f_1 and $\alpha = n^{-D}/400$ for f_2 . For both functions, $\alpha = n/2$ is used in SCR and each slice in SIR is set to contain about 200 samples. The subspace error in SCR and GCR converges almost in the order of $n^{-1/2}$ as expected. When g is monotonic, SIR yields the best performance. We will show in the next following examples that SIR can easily fail when g is not monotonic, while GCR can handle many more cases.

4.3 Example 3

The third example is

$$f(\mathbf{x}) = \sin\left(-\frac{\pi}{2} + \frac{\pi}{6} \sum_{i=1}^9 x_i\right) + x_{10}, \quad \mathbf{x} \in \mathbb{R}^{10}. \quad (24)$$

This function can be expressed as the model in (1) with $D = 10, d = 2, g(z_1, z_2) = \sin(-\frac{\pi}{2} + \frac{\pi}{2} z_1) + z_2, \mathbf{z} = \Phi^T \mathbf{x}, \Phi = [\mathbf{v}_1, \mathbf{v}_2]$ and

$$\mathbf{v}_1 = \frac{1}{3} \sum_{i=1}^9 \mathbf{e}_i, \quad \mathbf{v}_2 = \mathbf{e}_{10}.$$

Here $\mathbf{e}_i \in \mathbb{R}^D$ has 1 in the i th entry and 0 everywhere else. In this and the following examples, the \mathbf{x}_i 's are uniformly sampled from $[-1, 1]^D$, and the sample size varies such that $n = 10^3, 10^{3.3}, 10^{3.6}, 10^{3.9}, 10^{4.2}, 10^{4.5}$.

We first present the performance of GCR on noiseless data, i.e. $\sigma = 0$. In GCR, the parameter α should be chosen as $\alpha = Cn^{-1/D}$ according to (9). We set $C = 1, 1/10, 1/120, 1/1200, 1/12000$ and show the active subspace estimation error versus n in Figure 6(a) and the regression error versus n in Figure 6(b). Each error is averaged over 10 experiments. In log-log scale, the errors decay linearly as n increases with the same rate as long as C is not too large, as we expect. Our theory predicts the slopes in Figure 6(a) as -0.5 , which are almost matched by the slopes in Figure 6(a). The success

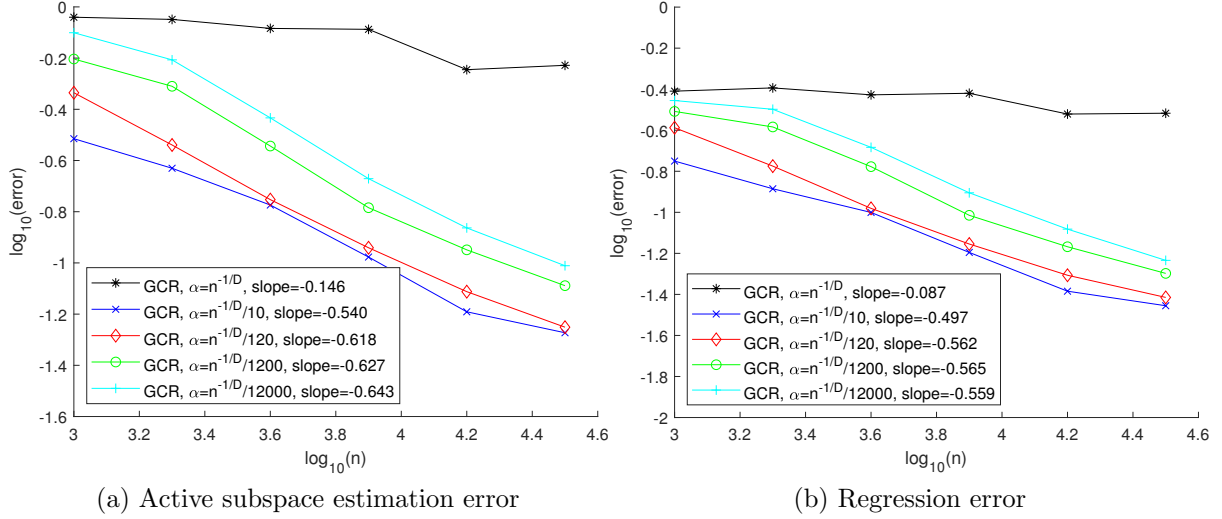


Figure 6: (Example 3 – performance of GCR without noise) Log-log plot of the active subspace estimation error (a) and the regression error (b) versus n , where $\alpha = Cn^{-1/D}$ in GCR with $C = 1, 1/10, 1/120, 1/1200, 1/12000$ respectively.

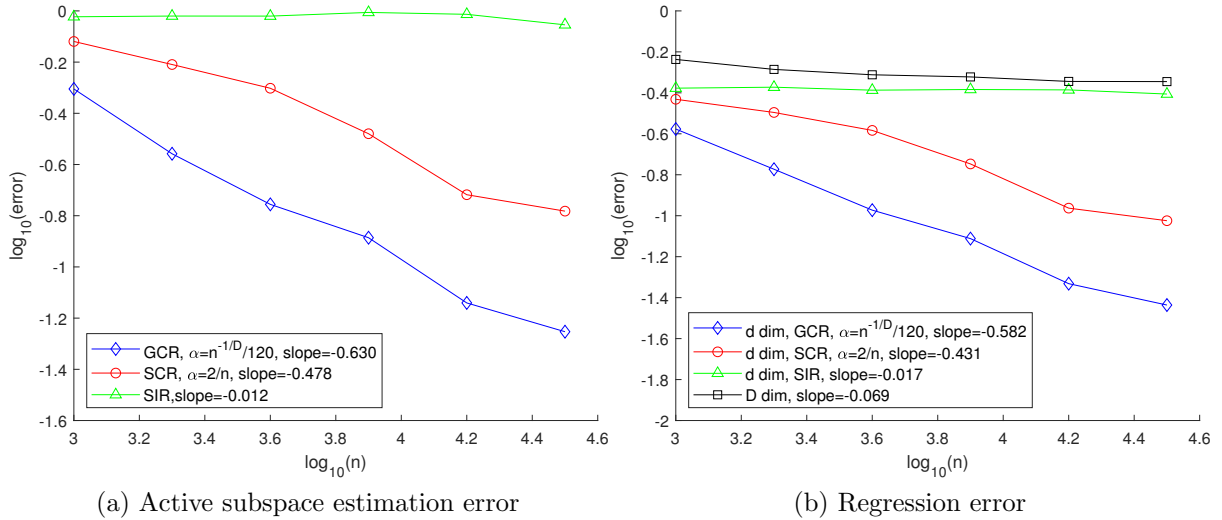


Figure 7: (Example 3 – Comparison of GCR, SCR and SIR without noise) Log-log plot of the active subspace estimation error (a) and the regression error (b) versus n by GCR, SCR and SIR. The black curve in (b) represents the regression error of f in \mathbb{R}^D without an estimation of the active subspace. GCR and SCR perform better than SIR, and GCR is the best. Estimating the active subspace greatly improves the rate of convergence in comparison with a direction regression in \mathbb{R}^D .

of GCR requires the condition (20), so GCR fails when C is too large, i.e. $C = 1$. The regression error is observed to converge in the order of $n^{-0.5}$ as long as C is not too large.

We next compare the performance of GCR, SCR and SIR with noiseless data. We set $\alpha = n^{-1/D}/120$ in GCR, and $\alpha = 2/n$ in SCR since it provides the best results among many choices. In SIR, each slice contains about 200 samples. We display the active subspace estimation error versus n in Figure 7(a) and the regression error versus n in Figure 7(b). Each error is the averaged error of 10 experiments. GCR and SCR perform

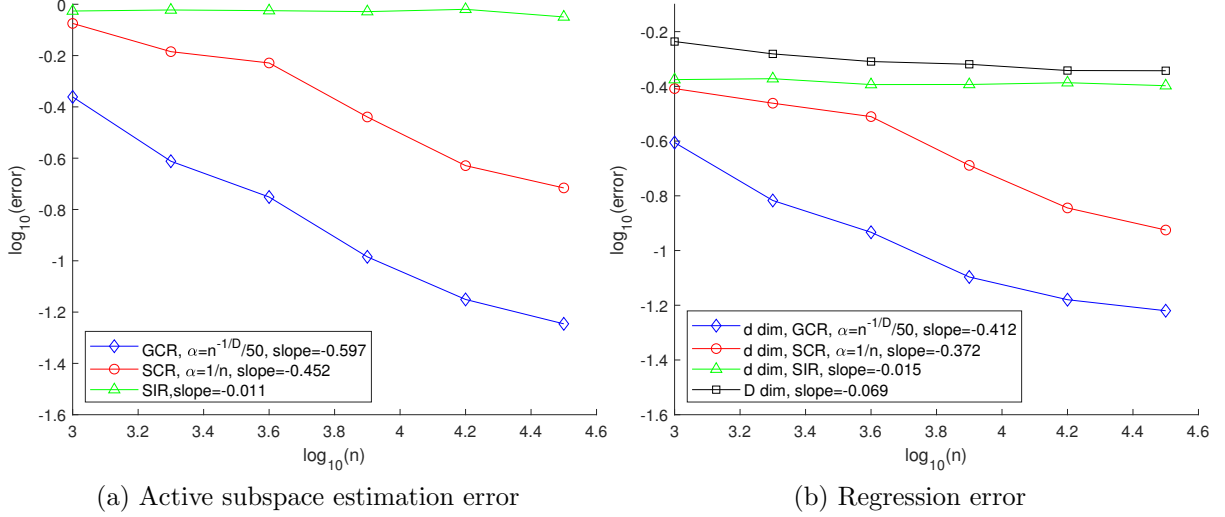


Figure 8: (Example 3 – Comparison of GCR, SCR and SIR with 5% noise) Log-log plot of the active subspace estimation error (a) and the regression error (b) versus n by GCR, SCR and SIR. The black curve in (b) represents the regression error of f in \mathbb{R}^D without an estimation of the active subspace. GCR and SCR perform better than SIR, and GCR is the best. Estimating the active subspace greatly improves the rate of convergence in comparison with a direction regression in \mathbb{R}^D .

better than SIR, and GCR is the best. Estimation of the active subspace greatly improves the rate of convergence in comparison with a direct regression in \mathbb{R}^D .

Results with 5% noise are shown in Figure 8. We set $\alpha = n^{-1/D}/50$ and $\alpha = 1/n$ in GCR and SCR. In SIR, each slice contains about 200 samples. We observe that GCR perform better than SCR and SIR.

We then compare GCR, SCR and SIR with heavy noise – 50%, 100% and 120% noise. Visualization of data along the \mathbf{v}_1 and \mathbf{v}_2 directions is shown in the first and second row of Figure 9. The third row shows the log-log plot of the active subspace estimation error by GCR, SCR and SIR versus n . Each error is averaged over 10 experiments. We observe that GCR is very robust against heavy noise – the active subspace estimation error converges in the order of $n^{-0.569}$ with 50% noise, and the rate slightly degrades in the presence of 100% and 120% noise. In comparison, SCR and SIR tend to fail when noise is heavy.

4.4 Example 4

The fourth example is

$$f(\mathbf{x}) = x_1^2 + (x_2 + x_3)^2, \quad \mathbf{x} \in \mathbb{R}^{10} \quad (25)$$

This function can be expressed as the model in (1) with $d = 2$, $D = 10$, $g(z_1, z_2) = z_1^2 + 2z_2^2$, $\mathbf{z} = \Phi^T \mathbf{x}$, $\Phi = [\mathbf{v}_1, \mathbf{v}_2]$ and

$$\mathbf{v}_1 = \mathbf{e}_1, \quad \mathbf{v}_2 = (\mathbf{e}_2 + \mathbf{e}_3)/\sqrt{2}.$$

This example is more challenging since f is not monotonic along both \mathbf{v}_1 and \mathbf{v}_2 directions.

Performance of GCR with $\alpha = Cn^{-1/D}$ where $C = 1/0.05, 1/0.5, 1/5, 1/50, 1/500$ on noiseless data is presented in Figure 10. The active subspace estimation error and the

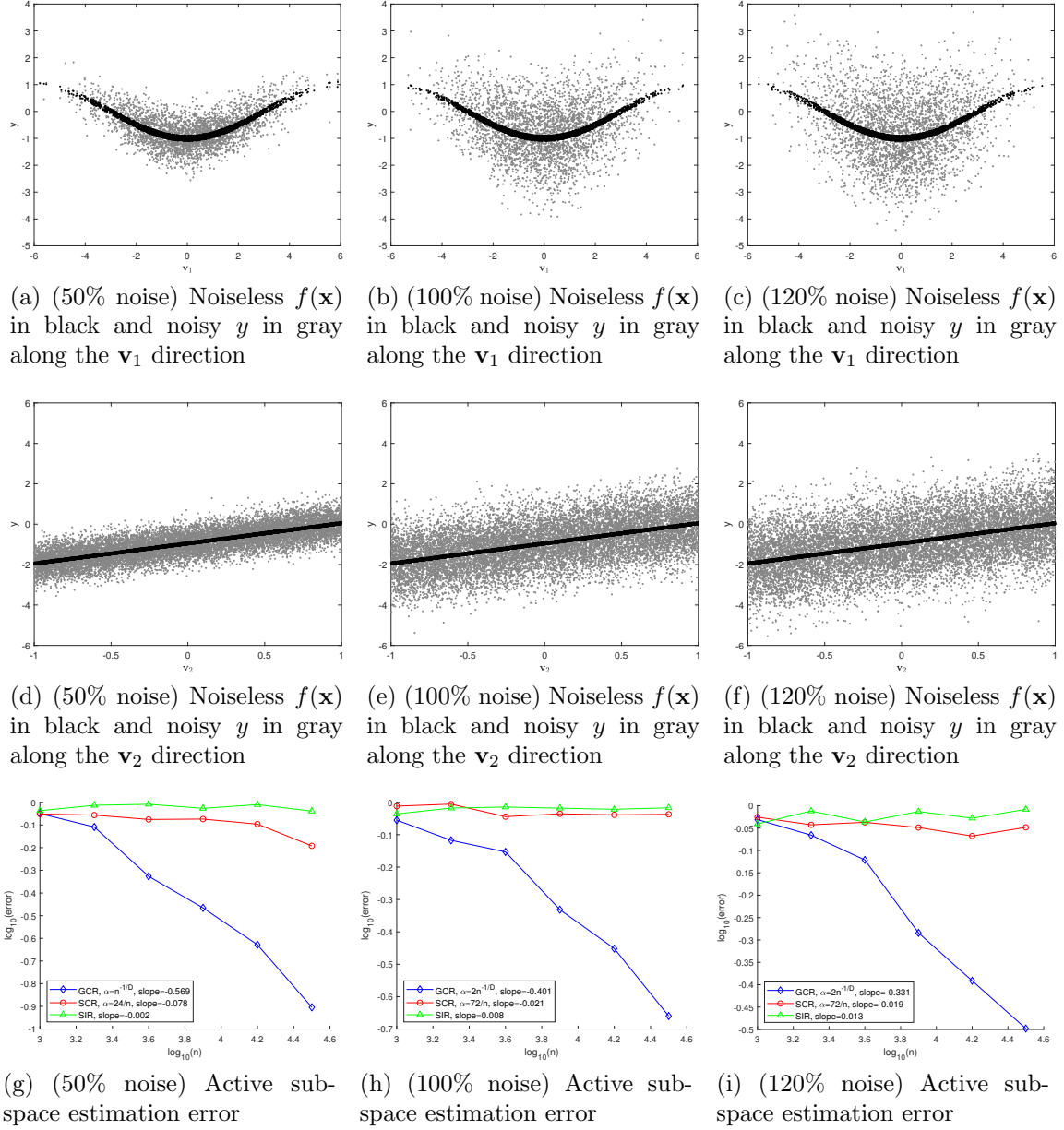


Figure 9: (Example 3 – Comparison of GCR, SCR and SIR with heavy noise: 50% noise in the left column, 100% in the middle column and 120% in the right column) The first row shows the visualization of the noiseless $f(\mathbf{x})$ in black and the noisy y in gray along the \mathbf{v}_1 direction while $-0.1 < x_{10} < 0.1$. The second row shows the visualization of the noiseless $f(\mathbf{x})$ in black and the noisy y in gray along the \mathbf{v}_2 direction while $-0.9 < \sum_1^9 x_i < 0.9$. The third row shows the log-log plot of the active subspace estimation error by GCR, SCR and SIR versus n .

regression error are shown in Figure 10 (a) and (b), respectively. Each error is averaged over 10 experiments. Our observation is similar to Example 2 that, in log-log scale, both errors decay linearly as n increases with the same slope, as long as C is not too large.

In Figure 11, we compare GCR, SCR and SIR with 5% noise. We set $\alpha = n^{-1/D}/50$ in GCR and $\alpha = 1/n$ in SCR. In SIR, each slice contains about 200 samples. We show the active subspace estimation error versus n in Figure 11 (a) and the regression error

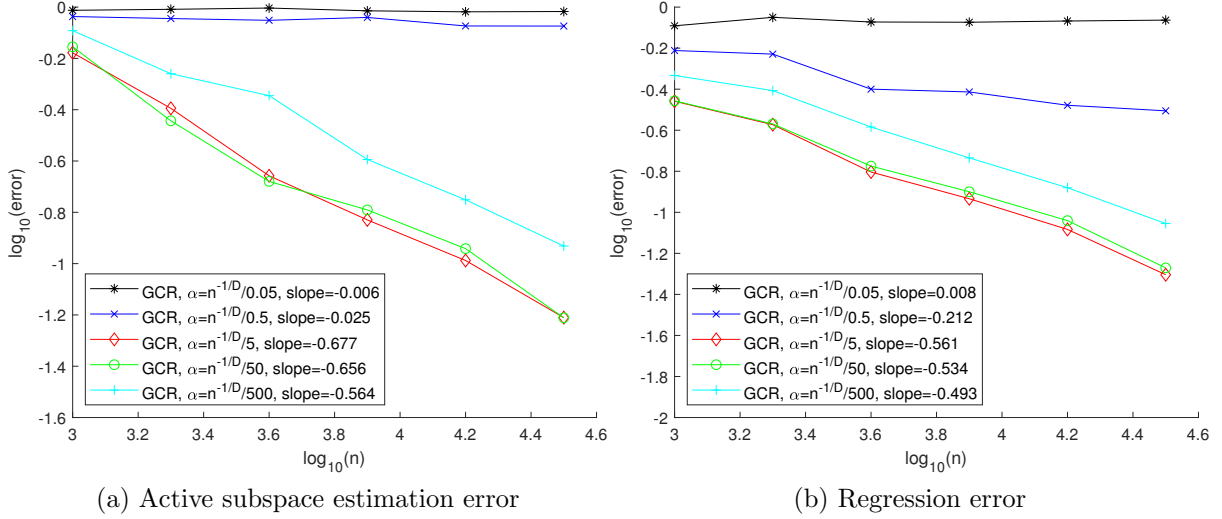


Figure 10: (Example 4 – performance of GCR without noise) Log-log plot of the active subspace estimation error (a) and the regression error (b) versus n , where $\alpha = Cn^{-1/D}$ in GCR with $C = 1/0.05, 1/0.5, 1/5, 1/50, 1/500$ respectively.

versus n in Figure 11 (b). Each error is averaged over 10 experiments. Among the three methods, GCR yields the smallest error and the fastest rate of convergence.

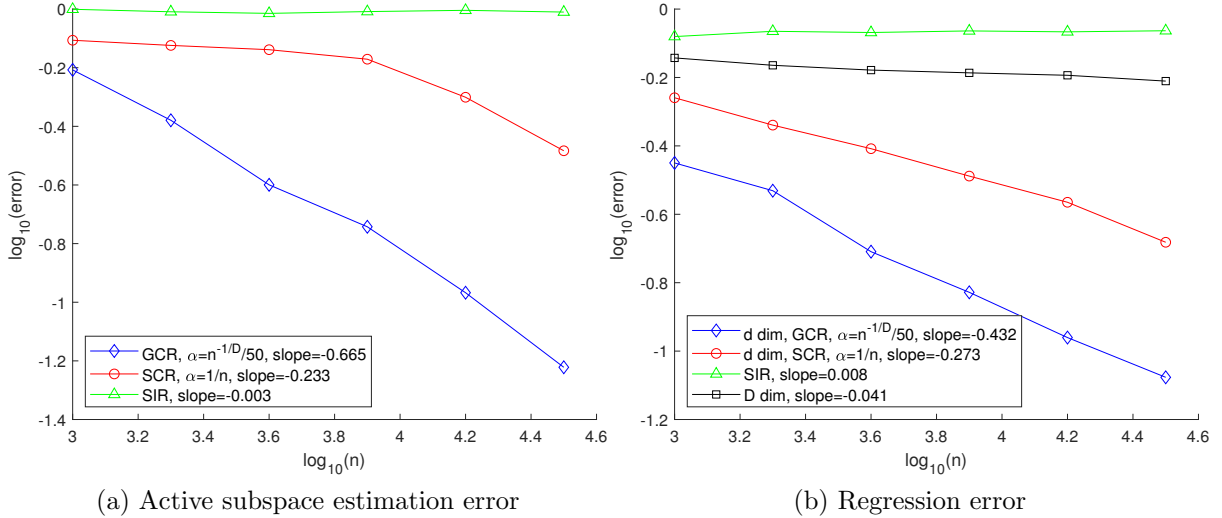


Figure 11: (Example 4 – Comparison of GCR, SCR and SIR with 5% noise) Log-log plot of the active subspace estimation error (a) and the regression error (b) versus n by GCR and SCR. The black curve in (b) represents the regression error of f in \mathbb{R}^D without an estimation of the active subspace. GCR performs better than SCR and SIR. Estimation of the active subspace greatly improves the rate of convergence in comparison with direction regression in \mathbb{R}^D .

Results with 50% noise are shown in Figure 12. We set $\alpha = n^{-1/D}$ in GCR and $\alpha = 24/n$ in SCR. In SIR, each slice contains about 200 samples. The noisy y (gray) and the noiseless $f(\mathbf{x})$ (black) are shown in Figure 12 (a) along the \mathbf{v}_1 direction with $-0.2 < x_2 + x_3 < 0.2$, and in Figure 12 (b) along the \mathbf{v}_2 direction with $0.1 < x_1 < x_2$. The active subspace estimation error by the three methods are displayed in Figure 12 (c).

Each error is averaged over 10 experiments. SCR and SIR perform poorly in this test, while GCR is very robust to heavy noise. The active subspace estimation error decays as $O(n^{-0.43})$, which is close to our prediction of $O(n^{-0.5})$.

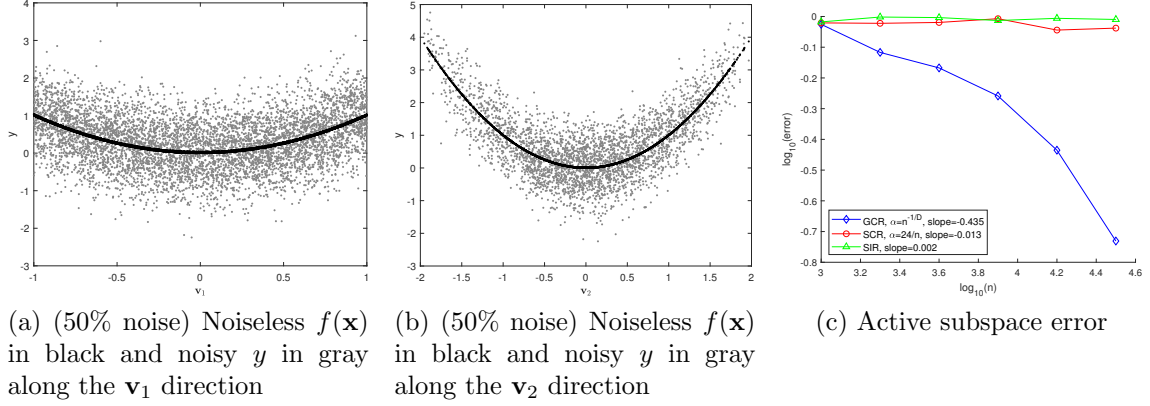


Figure 12: (Example 4 – Comparison of GCR, SCR and SIR with 50% noise) Visualization of noiseless $f(\mathbf{x})$ in black and the noisy y in gray along the \mathbf{v}_1 direction while $-0.2 < x_2 + x_3 < 0.2$ (a) and along the \mathbf{v}_2 direction while $-0.1 < x_1 < 0.1$ (b). (c) is the log-log plot of the active subspace estimation error versus n by GCR, SCR and SIR. GCR performs better than SCR and SIR. GCR is very robust against heavy noise.

4.5 Example 5

In Example 3 and 4, the function f can be written as a sum of two single index models. We next compare GCR, SCR and SIR on functions without such structures. Consider

$$f(\mathbf{x}) = 10 \sin\left(\frac{\pi}{5} (x_1 + 2(x_2 + x_3)^2)\right), \quad \mathbf{x} \in \mathbb{R}^{10}$$

which can be expressed in the model (1) with $D = 10, d = 2, g(z_1, z_2) = 10 \sin\left(\frac{\pi}{5} (z_1 + z_2^2)\right)$, $\mathbf{z} = \Phi^T \mathbf{x}, \Phi = [\mathbf{v}_1, \mathbf{v}_2]$ and

$$\mathbf{v}_1 = \mathbf{e}_1, \quad \mathbf{v}_2 = (\mathbf{e}_2 + \mathbf{e}_3)/\sqrt{2}.$$

We test GCR, SCR and SIR with 5% and 50% noise. The log-log plot of the active subspace estimation error versus n is displayed in Figure 13. Each error is averaged over 10 experiments. GCR has a convergence rate of $O(n^{-0.565})$ with 5% noise and $O(n^{-0.447})$ with 50% noise, which is robust to heavy noise and performs significantly better than SCR and SIR.

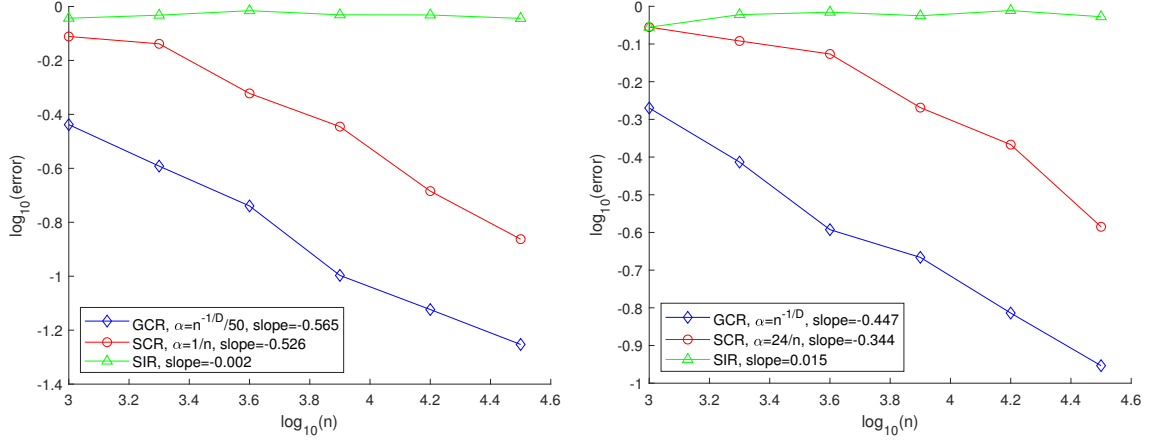
4.6 Example 6

Our last example is

$$f(\mathbf{x}) = 2x_1^2(x_2 + x_3)^2, \quad \mathbf{x} \in \mathbb{R}^{10}$$

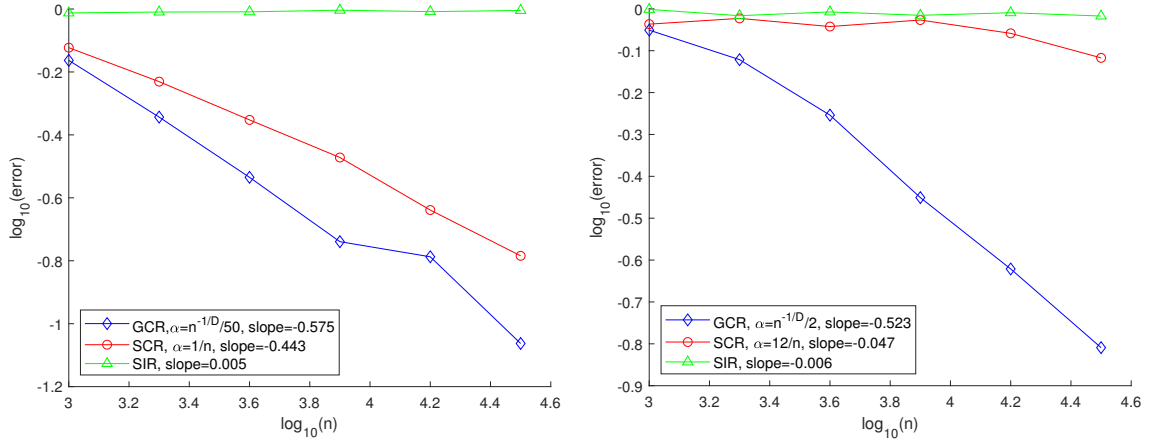
which can be expressed in the model (1) with $D = 10, d = 2, g(z_1, z_2) = 4z_1^2 z_2^2, \mathbf{z} = \Phi^T \mathbf{x}, \Phi = [\mathbf{v}_1, \mathbf{v}_2]$ and

$$\mathbf{v}_1 = \mathbf{e}_1, \quad \mathbf{v}_2 = (\mathbf{e}_2 + \mathbf{e}_3)/\sqrt{2}.$$



(a) (5% noise) Active subspace estimation error (b) (50% noise) Active subspace estimation error

Figure 13: (Example 5 – Comparison of GCR, SCR and SIR with 5% and 50% noise) Log-log plot of the active subspace estimation error versus n by GCR, SCR and SIR with 5% noise (a) and 50% noise (b).



(a) (5% noise) Active subspace estimation error (b) (50% noise) Active subspace estimation error

Figure 14: (Example 6 – Comparison of GCR, SCR and SIR with 5% and 50% noise.) Log-log plot of the active subspace estimation error versus n by GCR, SCR and SIR with 5% noise (a) and 50% noise (b). GCR performs better than SCR and SIR.

We test GCR, SCR and SIR with 5% and 50% noise. The log-log plot of the active subspace estimation error versus n is displayed in Figure 14. Each error is averaged over 10 experiments. GCR has a convergence rate of $O(n^{-0.575})$ with 5% noise and $O(n^{-0.523})$ with 50% noise, which is robust to heavy noise and performs significantly better than SCR and SIR.

5 Proof of main results

This section contains the proof of our main results in Section 3. Lemmas are proved in the Supplementary materials.

5.1 Proof of Theorem 1

Our central interest is to estimate the active subspace Φ . The estimator $\hat{\Phi}$ is obtained from the eigenvectors associated with the smallest d eigenvalues of $\hat{G}(\alpha, r)$. By Assumption 1 and Proposition 1, if $\alpha + \alpha_0 + 3\sigma^2 \leq \alpha_{\text{thresh}}$, the eigenvectors associated with the smallest d eigenvalues of $G(\alpha + \alpha_0 + 3\sigma^2)$ span the active subspace. To prove Theorem 1, we first show that $\|\hat{G}(\alpha, r) - G(\alpha + \alpha_0 + 3\sigma^2)\|$ is of $O(n^{-1/2})$ under Assumption 2(i), (ii), 3 and 4.

Proposition 2. *Let $\{\mathbf{x}_i\}_{i=1}^n$ be i.i.d. samples of the probability measure ρ , $\{y_i\}_{i=1}^n$ be sampled according to the model in (1), under Assumption 2(i), (ii), 3 and 4. For a fixed $\nu > 2$, if α and r are set according to (9), then for any $t > 0$,*

$$\mathbb{P}(\|\hat{G}(\alpha, r) - G(\alpha + \alpha_0 + 3\sigma^2)\| \geq t) \leq 2D \exp\left(\frac{-3t^2n}{64B^2(6B^2 + t)}\right) + 4n^{-(\nu-2)},$$

and when $\nu \geq 5/2$,

$$\mathbb{E}\|\hat{G}(\alpha, r) - G(\alpha + \alpha_0 + 3\sigma^2)\| \leq 16B^2 \left(\sqrt{2\log(2D)} + 2\right) n^{-\frac{1}{2}}.$$

For the proof of Proposition 2, we define the sampled covariance matrix $\bar{G}(\alpha)$ as

$$\bar{G}(\alpha) = \frac{1}{\bar{n}_\alpha} \sum_{\text{independent } (i,j): V_f(\mathbf{x}_i, \mathbf{x}_j) \leq \alpha} (\mathbf{x}_i - \mathbf{x}_j)(\mathbf{x}_i - \mathbf{x}_j)^T \quad (26)$$

where $\bar{n}_\alpha = \#\{\text{independent } (i, j) : V_f(\mathbf{x}_i, \mathbf{x}_j) \leq \alpha\}$. Here the sum is taken over a collection of independent matrices $(\mathbf{x}_i - \mathbf{x}_j)(\mathbf{x}_i - \mathbf{x}_j)^T$ satisfying $V_f(\mathbf{x}_i, \mathbf{x}_j) \leq \alpha$, while $\hat{G}(\alpha, r)$ sums over a collection of independent matrices satisfying $\hat{V}_y(\mathbf{x}_i, \mathbf{x}_j, r) \leq \alpha$. For a fixed α , $\bar{G}(\alpha)$ is not unique. Different collections of independent matrices $(\mathbf{x}_i - \mathbf{x}_j)(\mathbf{x}_i - \mathbf{x}_j)^T$ satisfying $V_f(\mathbf{x}_i, \mathbf{x}_j) \leq \alpha$ gives different $\bar{G}(\alpha)$. In practice, $V_f(\mathbf{x}_i, \mathbf{x}_j)$ can not be computed from samples, so is the matrix $\bar{G}(\alpha)$. It is defined for the proof only. To prove Proposition 2, we need the following three lemmas.

Lemma 2 (Concentration of $\bar{G}(\alpha)$ on $G(\alpha)$). *Let $\bar{G}(\alpha)$ be defined as (26) where the sum is taken over a collection of \bar{n}_α independent matrices $(\mathbf{x}_i - \mathbf{x}_j)(\mathbf{x}_i - \mathbf{x}_j)^T$ satisfying $V_f(\mathbf{x}_i, \mathbf{x}_j) \leq \alpha$. Under Assumption 2(i), if $\bar{n}_\alpha \geq 2\log(2D)/3$, then*

$$\mathbb{P}(\|\bar{G}(\alpha) - G(\alpha)\| \geq t) \leq 2D \exp\left(\frac{-3t^2\bar{n}_\alpha}{16B^2(6B^2 + t)}\right) \text{ for all } t \geq 0,$$

$$\mathbb{E}\|\bar{G}(\alpha) - G(\alpha)\| \leq 8B^2 \sqrt{\frac{2\log(2D)}{\bar{n}_\alpha}}.$$

Lemma 2 is proved via matrix Bernstein inequalities (see Supplementary materials B). We next show that if α_0 and r are chosen according to (8) and (9), then for any $\alpha > 0$, $\hat{G}(\alpha, r) = \bar{G}(\alpha + \alpha_0 + 3\sigma^2)$ with high probability.

Lemma 3. *Let $\{\mathbf{x}_i\}_{i=1}^n$ be i.i.d. samples from the probability measure ρ , and $\{y_i\}_{i=1}^n$ be sampled according to the model in (1), under Assumption 2 (i), (ii), 3 and 4. Let $\nu > 0$ and choose α_0 and r according to (8) and (9). For any $\alpha > 0$, if $\hat{G}(\alpha, r)$ sums over \hat{n}_α pairs of $(\mathbf{x}_i, \mathbf{x}_j)$ such that $\hat{V}_y(\mathbf{x}_i, \mathbf{x}_j, r) \leq \alpha$, then*

$$\hat{G}(\alpha, r) = \bar{G}(\alpha + \alpha_0 + 3\sigma^2)$$

with probability no less than $1 - 4\hat{n}_\alpha n^{-\nu}$.

The key of Lemma 3 is that, all $(\mathbf{x}_i, \mathbf{x}_j)$ pairs used in $\widehat{G}(\alpha, r)$ with $\widehat{V}_y(\mathbf{x}_i, \mathbf{x}_j, r) \leq \alpha$ also satisfy $V_f(\mathbf{x}_i, \mathbf{x}_j) \leq \alpha + \alpha_0 + 3\sigma^2$ with high probability. Thus $\widehat{G}(\alpha, r) = \bar{G}(\alpha + \alpha_0 + 3\sigma^2)$ with $\widehat{n}_{\alpha + \alpha_0 + 3\sigma^2} = \widehat{n}_\alpha$. Lemma 3 is proved in Supplementary materials C. Finally we show that \widehat{n}_α is $O(n)$ if α is chosen according to (9).

Lemma 4. *Let $\{\mathbf{x}_i\}_{i=1}^n$ be i.i.d. samples of the probability measure ρ , and $\{y_i\}_{i=1}^n$ be sampled according to the model in (1), under Assumption 2(i), (ii) and 3. Set α, r according to (9). For any $\nu > 2$, if n is sufficiently large such that $2(n/\log n)^{\frac{d}{2D}} \leq n$, then running Algorithm 1 gives rise to $\widehat{n}_\alpha \leq n/2$ and*

$$\mathbb{P}(\widehat{n}_\alpha \geq n/4) \geq 1 - 2n^{-(\nu-2)}.$$

Lemma 4 is proved in Supplementary materials D. Now we are ready to prove Proposition 2.

Proof of Proposition 2. Suppose $\widehat{G}(\alpha, r)$ sums over \widehat{n}_α independent matrices. By Lemma 4, one has $\widehat{n}_\alpha \leq n/2$, and $\widehat{n}_\alpha \geq n/4$ with probability no less than $1 - 2n^{-(\nu-2)}$. Denote the event

$$\mathcal{E} := \left(\widehat{G}(\alpha, r) = \bar{G}(\alpha + \alpha_0 + 3\sigma^2) \right) \cap \left(\widehat{n}_\alpha \geq \frac{n}{4} \right)$$

and its complement by \mathcal{E}^c . By Lemma 3, we have

$$\begin{aligned} \mathbb{P}(\mathcal{E}^c) &\leq 4\widehat{n}_\alpha n^{-\nu} + 2n^{-(\nu-2)} \leq 4n^{-(\nu-2)}, \\ \mathbb{P}(\mathcal{E}) &\geq 1 - 4n^{-(\nu-2)}. \end{aligned}$$

We first prove the probability bound. For every $t > 0$,

$$\begin{aligned} &\mathbb{P}(\|\widehat{G}(\alpha, r) - G(\alpha + \alpha_0 + 3\sigma^2)\| \geq t) \\ &\leq \mathbb{P}\left(\left[\|\widehat{G}(\alpha, r) - G(\alpha + \alpha_0 + 3\sigma^2)\| \geq t\right] \cap \mathcal{E}\right) + \mathbb{P}(\mathcal{E}^c) \\ &\leq \mathbb{P}\left(\|\widehat{G}(\alpha, r) - G(\alpha + \alpha_0 + 3\sigma^2)\| \geq t \mid \mathcal{E}\right) + \mathbb{P}(\mathcal{E}^c) \\ &\leq \mathbb{P}\left(\|\bar{G}(\alpha + \alpha_0 + 3\sigma^2) - G(\alpha + \alpha_0 + 3\sigma^2)\| \geq t \mid \mathcal{E}\right) + \mathbb{P}(\mathcal{E}^c) \\ &\leq 2D \exp\left(\frac{-3t^2\widehat{n}_\alpha}{16B^2(6B^2 + t)}\right) + 4n^{-(\nu-2)} \text{ according to Lemma 2} \\ &\leq 2D \exp\left(\frac{-3t^2n}{64B^2(6B^2 + t)}\right) + 4n^{-(\nu-2)} \text{ as } \widehat{n}_\alpha \geq n/4 \text{ conditional on } \mathcal{E}. \end{aligned}$$

We next prove the expectation bound by expressing

$$\begin{aligned} &\mathbb{E}\|\widehat{G}(\alpha, r) - G(\alpha + \alpha_0 + 3\sigma^2)\| \\ &= \mathbb{E}\left(\|\widehat{G}(\alpha, r) - G(\alpha + \alpha_0 + 3\sigma^2)\| \mid \mathcal{E}\right) \mathbb{P}(\mathcal{E}) + \mathbb{E}\left(\|\widehat{G}(\alpha, r) - G(\alpha + \alpha_0 + 3\sigma^2)\| \mid \mathcal{E}^c\right) \mathbb{P}(\mathcal{E}^c). \end{aligned}$$

The first term follows from Lemma 2 such that

$$\begin{aligned} &\mathbb{E}\left(\|\widehat{G}(\alpha, r) - G(\alpha + \alpha_0 + 3\sigma^2)\| \mid \mathcal{E}\right) \\ &= \mathbb{E}\left(\|\bar{G}(\alpha + \alpha_0 + 3\sigma^2) - G(\alpha + \alpha_0 + 3\sigma^2)\| \mid \mathcal{E}\right) \leq 16B^2 \sqrt{\frac{2\log(2D)}{n}}. \end{aligned}$$

As $\|\mathbf{x}\| \leq B$, the second term satisfies $\mathbb{E} \left(\|\widehat{G}(\alpha, r) - G(\alpha + \alpha_0 + 3\sigma^2)\| \mid \mathcal{E}^c \right) \mathbb{P}(\mathcal{E}^c) \leq 8B^2 \mathbb{P}(\mathcal{E}^c) \leq 32B^2 n^{-(\nu-2)}$. Therefore, when ν is chosen such that $\nu \geq \frac{5}{2}$,

$$\begin{aligned} \mathbb{E} \|\widehat{G}(\alpha, r) - G(\alpha + \alpha_0 + 3\sigma^2)\| &\leq 16B^2 \sqrt{\frac{2 \log(2D)}{n}} + 32n^{-(\nu-2)} B^2 \\ &\leq 16B^2 \left(\sqrt{2 \log(2D)} + 2 \right) n^{-\frac{1}{2}}. \end{aligned}$$

□

We next use Davis-Kahan theorem (Lemma 5) and Weyl theorem (Lemma 6) to make a connection between $\|\text{Proj}_{\widehat{\Phi}} - \text{Proj}_{\Phi}\|$ and $\|\widehat{G}(\alpha, r) - G(\alpha + \alpha_0 + 3\sigma^2)\|$.

Lemma 5 (Davis-Kahan [10, 35]). *Let $G, \widehat{G} \in \mathbb{C}^{D \times D}$ be two Hermitian matrices with eigenvalues $\lambda_j, \widehat{\lambda}_j, j = 1, \dots, D$ in non-increasing order. Let the columns of Φ and $\widehat{\Phi}$ consist of orthonormal bases of the eigenspaces associated with the largest d eigenvalues of G and \widehat{G} respectively. Suppose $\widehat{\lambda}_{d+1} < \lambda_d$, then*

$$\|\text{Proj}_{\widehat{\Phi}} - \text{Proj}_{\Phi}\| \leq \frac{\|\widehat{G} - G\|}{\lambda_d - \widehat{\lambda}_{d+1}}. \quad (27)$$

Lemma 6 (Weyl [39]). *$G, \widehat{G} \in \mathbb{C}^{D \times D}$ be two Hermitian matrices with eigenvalues $\lambda_j, \widehat{\lambda}_j, j = 1, \dots, D$ in non-increasing order. Then*

$$|\lambda_j - \widehat{\lambda}_j| \leq \|\widehat{G} - G\|, \forall j = 1, \dots, D. \quad (28)$$

Now we are ready to prove Theorem 1.

Proof of Theorem 1. First note that the column space of $\widehat{\Phi}$ is the one spanned by eigenvectors corresponding to the largest d eigenvalues of $I - \widehat{G}(\alpha, r)$. The same is true for Φ and $I - G(\alpha + \alpha_0 + 3\sigma^2)$. Let the eigenvalues of $G(\alpha + \alpha_0 + 3\sigma^2)$ be $\{\lambda_j\}_{j=1}^D$. Assumption 1, 2(iii) and Proposition 1 imply $\lambda_{D-d} - \lambda_{D-d+1} \geq C_0 - \phi(\alpha + \alpha_0 + 3\sigma^2)$. Combining Lemma 5 and Lemma 6 with $G = G(\alpha + \alpha_0 + 3\sigma^2)$ and $\widehat{G} = \widehat{G}(\alpha, r)$ gives rise to

$$\begin{aligned} \|\text{Proj}_{\widehat{\Phi}} - \text{Proj}_{\Phi}\| &\leq \frac{\|(I - \widehat{G}(\alpha, r)) - (I - G(\alpha + \alpha_0 + 3\sigma^2))\|}{(1 - \lambda_{D-d+1}) - (1 - \lambda_{D-d}) - \|\widehat{G}(\alpha, r) - G(\alpha + \alpha_0 + 3\sigma^2)\|} \\ &\leq \frac{\|\widehat{G}(\alpha, r) - G(\alpha + \alpha_0 + 3\sigma^2)\|}{C_0 - \phi(\alpha + \alpha_0 + 3\sigma^2) - \|\widehat{G}(\alpha, r) - G(\alpha + \alpha_0 + 3\sigma^2)\|} \end{aligned}$$

Notice that $\|\text{Proj}_{\widehat{\Phi}} - \text{Proj}_{\Phi}\| \leq 2$. For any $0 < t < 2$, a sufficient condition to guarantee $\|\text{Proj}_{\widehat{\Phi}} - \text{Proj}_{\Phi}\| \leq t$ is $\|\widehat{G}(\alpha, r) - G(\alpha + \alpha_0 + 3\sigma^2)\| \leq t[C_0 - \phi(\alpha + \alpha_0 + 3\sigma^2)]/(1+t)$ together with $C_0 - \phi(\alpha + \alpha_0 + 3\sigma^2) - \|\widehat{G}(\alpha, r) - G(\alpha + \alpha_0 + 3\sigma^2)\| > 0$. Since $0 < t < 2$, we can express this sufficient condition as

$$\|\widehat{G}(\alpha, r) - G(\alpha + \alpha_0 + 3\sigma^2)\| \leq [C_0 - \phi(\alpha + \alpha_0 + 3\sigma^2)]t/3.$$

Therefore, for any $t \in (0, 2)$,

$$\mathbb{P} \left\{ \|\text{Proj}_{\widehat{\Phi}} - \text{Proj}_{\Phi}\| \geq t \right\} \leq \mathbb{P} \left\{ \|\widehat{G}(\alpha, r) - G(\alpha + \alpha_0 + 3\sigma^2)\| \geq [C_0 - \phi(\alpha + \alpha_0 + 3\sigma^2)]t/3 \right\}.$$

Combining the inequality above and Proposition 2 gives rise to (21).

□

5.2 Proof of Corollary 1

Lemma 7. *If $X \geq 0$ is a random variable such that*

$$\mathbb{P}(X \geq t) \leq Ae^{-\frac{at^2}{b+ct}}, \quad \forall t \geq 0$$

for some $a > 0, b > 0, c > 0$, then

$$\mathbb{E}(X^2) \leq \frac{b}{a}(\log(A) + A + 1) + \frac{4Ac^2}{a^2}. \quad (29)$$

Lemma 7 is proved in Supplementary materials E. The proof of Corollary 1 is based on Lemma 7.

Proof of Corollary 1. Combining Theorem 1 and Lemma 7 gives rise to

$$\begin{aligned} \mathbb{E}\|\text{Proj}_{\hat{\Phi}} - \text{Proj}_{\Phi}\|^2 &= \int_0^{+\infty} t\mathbb{P}(\|\text{Proj}_{\hat{\Phi}} - \text{Proj}_{\Phi}\| \geq t)dt \\ &= \int_0^{+\infty} 2tD \exp\left(\frac{-(C_0 - \phi(\alpha + \alpha_0 + 3\sigma^2))^2 nt^2}{64B^2(18B^2 + (C_0 - \phi(\alpha + \alpha_0 + 3\sigma^2))t)}\right) + \int_0^{+\infty} 4tn^{-(\nu-2)}dt \\ &\leq \int_0^{+\infty} 2tD \exp\left(\frac{-(C_0 - \phi(\alpha + \alpha_0 + 3\sigma^2))^2 nt^2}{64B^2(18B^2 + (C_0 - \phi(\alpha + \alpha_0 + 3\sigma^2))t)}\right) dt \\ &\quad + \int_0^2 4tn^{-(\nu-2)}dt \quad \text{since } \|\text{Proj}_{\hat{\Phi}} - \text{Proj}_{\Phi}\| \leq 2 \\ &\leq \frac{C_5}{C_4}(\log(2D) + 2D + 1)n^{-1} + \frac{8DC_6^2}{C_4^2}n^{-2} + 8n^{-(\nu-2)} \quad \text{by Lemma 7} \\ &\leq \frac{C_5}{C_4}(\log(2D) + 2D + 1)n^{-1} + \frac{8DC_6^2}{C_4^2}n^{-2} + 8n^{-1} \quad \text{since } \nu \geq 3 \\ &\leq C_7/n \end{aligned}$$

where C_4, C_5, C_6, C_7 are defined in (17). □

5.3 Proof of Theorem 2

In model (10), $\{\mathbf{z}_i\}_{i=n+1}^{2n}$ are independently sampled from the marginal distribution of ρ on the subspace spanned by $\hat{\Phi}$. Denote this marginal distribution by μ . For any set $\Omega \subset \mathbb{R}^d$, $\mu(\Omega) = \rho(\{\mathbf{x} \in \mathbb{R}^D | \hat{\Phi}^T \mathbf{x} \in \Omega\})$. According to (18), the regression error of f crucially depends on the estimation error of g , which is established in the following lemma.

Lemma 8. *Let $\{\mathbf{z}_i\}_{i=n+1}^{2n}$ be i.i.d. sampled from a probability measure μ such that $\text{supp}(\mu) \subseteq [-B, B]^d$ and $\{y_i\}_{i=n+1}^{2n}$ follows the model in (10). Let \hat{g} be the estimator in (15) with polynomial order $k = \lfloor s + 1 \rfloor - 1$. Under Assumption 2(i), 3, 4, we have*

$$\begin{aligned} &\mathbb{E} \int |\hat{g}(\mathbf{z}) - g(\mathbf{z})|^2 \mu(d\mathbf{z}) \\ &\leq 2c \cdot \max(\sigma^2 + b_{\text{bias}}^2, 2M^2 + 2b_{\text{bias}}^2) \frac{\binom{d+k}{d} K^d \log n}{n} + \frac{4C_g^2 B^{2s} d^{s+k}}{(k!)^2 K^{2s}} + 6b_{\text{bias}}^2. \end{aligned} \quad (30)$$

where c is a universal constant and b_{bias}^2 is defined in (13).

Lemma 8 is proved in Supplementary materials F by classical results in nonparametric regression [16, 33, 14, 9]. The proof of Theorem 2 is given below.

Proof of Theorem 2. From (18), (19) and the fact that $\|\mathbf{x}\| \leq B$, one has

$$|\hat{f}(\mathbf{x}) - f(\mathbf{x})|^2 \leq 4dL_g^2 B^2 \|\text{Proj}_{\hat{\Phi}} - \text{Proj}_{\Phi}\|^2 + 2|\hat{g}(\hat{\Phi}^T \mathbf{x}) - g(\hat{\Phi}^T \mathbf{x})|^2. \quad (31)$$

We use $\mathbb{E}_{\{(\mathbf{x}_i, y_i)\}_{i=1}^{2n}}(h(\mathbf{x}))$ to denote the expectation of $h(\mathbf{x})$ with respect to the joint distribution of $\{(\mathbf{x}_i, y_i)\}_{i=1}^{2n}$. Then

$$\begin{aligned} & \mathbb{E}_{\{(\mathbf{x}_i, y_i)\}_{i=1}^{2n}} (\|\hat{f}(\mathbf{x}) - f(\mathbf{x})\|_{L^2(\rho)}^2) \\ &= \mathbb{E}_{\{(\mathbf{x}_i, y_i)\}_{i=1}^{2n}} \left(\int |\hat{f}(\mathbf{x}) - f(\mathbf{x})|^2 \rho(d\mathbf{x}) \right) \\ &\leq 4dL_g^2 B^2 \mathbb{E}_{\{(\mathbf{x}_i, y_i)\}_{i=1}^n} (\|\text{Proj}_{\hat{\Phi}} - \text{Proj}_{\Phi}\|^2) \\ &\quad + 2 \mathbb{E}_{\{(\mathbf{x}_i, y_i)\}_{i=1}^n} \left(\mathbb{E}_{\{(\mathbf{x}_i, y_i)\}_{i=n+1}^{2n}} \left(\int |\hat{g}(\hat{\Phi}^T \mathbf{x}) - g(\hat{\Phi}^T \mathbf{x})|^2 \rho(d\mathbf{x}) \right) \middle| \{(\mathbf{x}_i, y_i)\}_{i=1}^n \right). \end{aligned}$$

Corollary 1 gives an estimate of the first term

$$\mathbb{E}_{\{(\mathbf{x}_i, y_i)\}_{i=1}^n} (\|\text{Proj}_{\hat{\Phi}} - \text{Proj}_{\Phi}\|^2) \leq \frac{C_7}{n}. \quad (32)$$

The second term in (31) can be estimated through Lemma 8:

$$\begin{aligned} & \mathbb{E}_{\{(\mathbf{x}_i, y_i)\}_{i=1}^n} \left(\mathbb{E}_{\{(\mathbf{x}_i, y_i)\}_{i=n+1}^{2n}} \left(\int |\hat{g}(\hat{\Phi}^T \mathbf{x}) - g(\hat{\Phi}^T \mathbf{x})|^2 \rho(d\mathbf{x}) \right) \middle| \{(\mathbf{x}_i, y_i)\}_{i=1}^n \right) \\ &= \mathbb{E}_{\{(\mathbf{x}_i, y_i)\}_{i=1}^n} \left(\mathbb{E}_{\{(\mathbf{z}_i, y_i)\}_{i=n+1}^{2n}} \left(\int |\hat{g}(\mathbf{z}) - g(\mathbf{z})|^2 \mu(d\mathbf{z}) \right) \middle| \{(\mathbf{x}_i, y_i)\}_{i=1}^n \right) \\ &\leq \mathbb{E}_{\{(\mathbf{x}_i, y_i)\}_{i=1}^n} \left[2c \cdot \max(\sigma^2 + b_{\text{bias}}^2, 2M^2 + 2b_{\text{bias}}^2) \frac{\binom{d+k}{d} K^d \log n}{n} \right. \\ &\quad \left. + \frac{4C_g^2 B^{2s} d^{s+k}}{(k!)^2 K^{2s}} + 6b_{\text{bias}}^2 \middle| \{(\mathbf{x}_i, y_i)\}_{i=1}^n \right] \\ &\leq 2c \cdot \max \left(\sigma^2 + \mathbb{E}_{\{(\mathbf{x}_i, y_i)\}_{i=1}^n} b_{\text{bias}}^2, 2M^2 + 2 \mathbb{E}_{\{(\mathbf{x}_i, y_i)\}_{i=1}^n} b_{\text{bias}}^2 \right) \frac{\binom{d+k}{d} K^d \log n}{n} \\ &\quad + \frac{4C_g^2 B^{2s} d^{s+k}}{(k!)^2 K^{2s}} + 6 \mathbb{E}_{\{(\mathbf{x}_i, y_i)\}_{i=1}^n} b_{\text{bias}}^2 \\ &\leq C \left(\frac{\max(\sigma^2 + 2C_8 n^{-1}, 2M^2 + 4C_8 n^{-1}) \log n}{n} \right)^{\frac{2s}{2s+d}} + \frac{12C_8}{n}, \quad (33) \end{aligned}$$

where C_8 is defined in (17) and $C = 2c \binom{d+k}{d} + \frac{4C_g^2 B^{2s} d^{s+k}}{(k!)^2}$ independent of n . The last inequality in (33) results from

$$\mathbb{E}_{\{(\mathbf{x}_i, y_i)\}_{i=1}^n} b_{\text{bias}}^2 \leq 2dC_7 L_g^2 B^2 n^{-1}$$

by Corollary 1 and K chosen according to (16). Finally Combining (32) and (33) gives rise to (23). \square

6 Conclusion

In this work, we combine GCR and piecewise polynomial approximations to estimate a high-dimensional function which varies along a low-dimensional active subspace. When the sample size n is sufficiently large and the noise level is sufficiently low, the mean squared estimation error for the active subspace is $O(n^{-1})$ and the mean squared regression error is $O((n/\log n)^{-\frac{2s}{2s+d}})$. These results are verified by numerical experiments.

Acknowledgement

Wenjing Liao's research is supported by NSF DMS 1818751. Both authors are grateful to Alessandro Lanteri, Mauro Maggioni and Stefano Vigogna for pointing out the noise bias in the regression model (10), which was not taken care of in the first version of this manuscript. This problem has been fixed in the current version.

References

- [1] I. Babuška, R. Temponet, and G. E. Zouraris. Galerkin finite element approximations of stochastic elliptic partial differential equations. *SIAM Journal on Numerical Analysis*, 2004.
- [2] E. Bura and R. D. Cook. Estimating the structural dimension of regressions via parametric inverse regression. *Journal of the Royal Statistical Society. Series B: Statistical Methodology*, 2001.
- [3] E. Bura and R. M. Pfeiffer. Graphical methods for class prediction using dimension reduction techniques on DNA microarray data. *Bioinformatics*, 2003.
- [4] C. Chesneau. Regression with random design: a minimax study. *Statistics & probability letters*, 77(1):40–53, 2007.
- [5] A. Cohen, I. Daubechies, R. DeVore, G. Kerkyacharian, and D. Picard. Capturing Ridge Functions in High Dimensions from Point Queries. *Constructive Approximation*, 2012.
- [6] P. G. Constantine, E. Dow, and Q. Wang. Active subspace methods in theory and practice: applications to kriging surfaces. *SIAM Journal on Scientific Computing*, 36(4):A1500–A1524, 2014.
- [7] P. G. Constantine, B. Zaharatos, and M. Campanelli. Discovering an active subspace in a single-diode solar cell model. *Statistical Analysis and Data Mining: The ASA Data Science Journal*, 8(5-6):264–273, 2015.
- [8] R. D. Cook and S. Weisberg. Sliced inverse regression for dimension reduction: Comment. *Journal of the American Statistical Association*, 86(414):328–332, 1991.
- [9] D. D. Cox et al. Approximation of least squares regression on nested subspaces. *The Annals of Statistics*, 16(2):713–732, 1988.

- [10] C. Davis and W. M. Kahan. The rotation of eigenvectors by a perturbation. iii. *SIAM Journal on Numerical Analysis*, 7(1):1–46, 1970.
- [11] M. Fornasier, K. Schnass, and J. Vybiral. Learning Functions of Few Arbitrary Linear Parameters in High Dimensions. *Foundations of Computational Mathematics*, 2012.
- [12] W. K. Fung, X. He, L. Liu, and P. Shi. Dimension reduction based on canonical correlation. *Statistica Sinica*, pages 1093–1113, 2002.
- [13] S. Gaïffas, G. Lecué, et al. Optimal rates and adaptation in the single-index model using aggregation. *Electronic journal of statistics*, 1:538–573, 2007.
- [14] S. Geer, S. van de Geer, R. Gill, B. Ripley, S. Ross, B. Silverman, and M. Stein. *Empirical Processes in M-Estimation*. Cambridge Series in Statistical and Probabilistic Mathematics. Cambridge University Press, 2000.
- [15] P. E. Gill, W. Murray, and M. H. Wright. Practical optimization. *London: Academic Press, 1981*, 1981.
- [16] L. Györfi, M. Kohler, A. Krzyzak, and H. Walk. *A Distribution-Free theory of Nonparametric Regression*. Springer Science & Business Media, 2006.
- [17] W. Härdle and T. M. Stoker. Investigating smooth multiple regression by the method of average derivatives. *Journal of the American Statistical Association*, 1989.
- [18] W. Härdle and A. B. Tsybakov. How sensitive are average derivatives? *Journal of Econometrics*, 58(1-2):31–48, 1993.
- [19] W. Hoeffding. Probability inequalities for sums of bounded random variables. In *The Collected Works of Wassily Hoeffding*, pages 409–426. Springer, 1994.
- [20] M. Hristache, A. Juditsky, J. Polzehl, and V. Spokoiny. Structure adaptive approach for dimension reduction. *Annals of Statistics*, 2001.
- [21] H. Ichimura. Semiparametric least squares (sls) and weighted sls estimation of single-index models. *Journal of Econometrics*, 58(1-2):71–120, 1993.
- [22] H. Kim, P. Howland, and H. Park. Dimension reduction in text classification with support vector machines. *Journal of Machine Learning Research*, 6(Jan):37–53, 2005.
- [23] A. Lanteri, M. Maggioni, and S. Vigogna. Conditional regression for single-index models. *arXiv preprint arXiv:2002.10008*, 2020.
- [24] O. Lepski, N. Serdyukova, et al. Adaptive estimation under single-index constraint in a regression model. *The Annals of Statistics*, 42(1):1–28, 2014.
- [25] B. Li. *Sufficient dimension reduction: Methods and applications with R*. Chapman and Hall/CRC, 2018.
- [26] B. Li and S. Wang. On directional regression for dimension reduction. *Journal of the American Statistical Association*, 102(479):997–1008, 2007.
- [27] B. Li, H. Zha, F. Chiaromonte, et al. Contour regression: a general approach to dimension reduction. *The Annals of Statistics*, 33(4):1580–1616, 2005.

- [28] K. C. Li. Sliced inverse regression for dimension reduction. *Journal of the American Statistical Association*, 1991.
- [29] W. Liao and M. Maggioni. Adaptive geometric multiscale approximations for intrinsically low-dimensional data. *Journal of Machine Learning Research*, 20(98):1–63, 2019.
- [30] Y. Ma and L. Zhu. A review on dimension reduction. *International Statistical Review*, 2013.
- [31] R. M. Pfeiffer and E. Bura. A model free approach to combining biomarkers. *Biometrical Journal*, 2008.
- [32] R. M. Pfeiffer, L. Forzani, and E. Bura. Sufficient dimension reduction for longitudinally measured predictors. *Statistics in Medicine*, 2012.
- [33] D. Pollard. *Convergence of Stochastic Processes*. Clinical Perspectives in Obstetrics and Gynecology. Springer New York, 1984.
- [34] J. L. Powell, J. H. Stock, and T. M. Stoker. Semiparametric Estimation of Index Coefficients. *Econometrica*, 1989.
- [35] W. G. Stewart and J.-G. Sun. *Matrix perturbation theory*. Academic Press, 1990.
- [36] J. A. Tropp. User-friendly tools for random matrices: An introduction. Technical report, California Institute of Technology Division of Engineering and Applied Science, 2012.
- [37] A. B. Tsybakov. *Introduction to Nonparametric Estimation*. Springer-Verlag New York, 2009.
- [38] L. Wasserman. *All of nonparametric statistics*. Springer Science & Business Media, 2006.
- [39] H. Weyl. Das asymptotische verteilungsgesetz der eigenwerte linearer partieller differentialgleichungen (mit einer anwendung auf die theorie der hohlraumstrahlung). *Mathematische Annalen*, 71(4):441–479, 1912.
- [40] Y. Xia, H. Tong, W. K. Li, and L.-X. Zhu. An adaptive estimation of dimension reduction space. *Journal of the Royal Statistical Society: Series B (Statistical Methodology)*, 64(3):363–410, 2002.
- [41] K. Zhou, J. C. Doyle, K. Glover, et al. *Robust and optimal control*, volume 40. Prentice hall New Jersey, 1996.
- [42] L. X. Zhu and K. T. Fang. Asymptotics for kernel estimate of sliced Inverse regression. *Annals of Statistics*, 1996.
- [43] L. X. Zhu, M. Ohtaki, and Y. Li. On hybrid methods of inverse regression-based algorithms. *Computational statistics & data analysis*, 51(5):2621–2635, 2007.

Supplemental Materials for Learning functions varying along an active subspace

A Proof of Proposition 1

Proof of Proposition 1. By expressing $\tilde{\mathbf{x}} - \mathbf{x} = \text{Proj}_{\mathcal{S}_\Phi}(\tilde{\mathbf{x}} - \mathbf{x}) + \text{Proj}_{\mathcal{S}_\Phi^\perp}(\tilde{\mathbf{x}} - \mathbf{x})$, we can write the covariance matrix as

$$\begin{aligned} & \mathbb{E} [(\tilde{\mathbf{x}} - \mathbf{x})(\tilde{\mathbf{x}} - \mathbf{x})^T] \\ &= \mathbb{E} \left[\text{Proj}_{\mathcal{S}_\Phi}(\tilde{\mathbf{x}} - \mathbf{x}) [\text{Proj}_{\mathcal{S}_\Phi}(\tilde{\mathbf{x}} - \mathbf{x})]^T \right] + \mathbb{E} \left[\text{Proj}_{\mathcal{S}_\Phi^\perp}(\tilde{\mathbf{x}} - \mathbf{x}) [\text{Proj}_{\mathcal{S}_\Phi^\perp}(\tilde{\mathbf{x}} - \mathbf{x})]^T \right] \\ & \quad + \mathbb{E} \left[\text{Proj}_{\mathcal{S}_\Phi}(\tilde{\mathbf{x}} - \mathbf{x}) [\text{Proj}_{\mathcal{S}_\Phi^\perp}(\tilde{\mathbf{x}} - \mathbf{x})]^T \right] + \mathbb{E} \left[\text{Proj}_{\mathcal{S}_\Phi^\perp}(\tilde{\mathbf{x}} - \mathbf{x}) [\text{Proj}_{\mathcal{S}_\Phi}(\tilde{\mathbf{x}} - \mathbf{x})]^T \right] \\ &= \Phi \mathbb{E} [\Phi^T(\tilde{\mathbf{x}} - \mathbf{x})(\tilde{\mathbf{x}} - \mathbf{x})^T \Phi] \Phi^T + \Psi \mathbb{E} [\Psi^T(\tilde{\mathbf{x}} - \mathbf{x})(\tilde{\mathbf{x}} - \mathbf{x})^T \Psi] \Psi^T \\ & \quad + \Phi \mathbb{E} [\Phi^T(\tilde{\mathbf{x}} - \mathbf{x})(\tilde{\mathbf{x}} - \mathbf{x})^T \Psi] \Psi^T + \Psi \mathbb{E} [\Psi^T(\tilde{\mathbf{x}} - \mathbf{x})(\tilde{\mathbf{x}} - \mathbf{x})^T \Phi] \Phi^T \end{aligned}$$

where the columns of Ψ form an orthonormal basis of \mathcal{S}_Φ^\perp .

We next prove $\mathbb{E} [\Psi^T(\tilde{\mathbf{x}} - \mathbf{x})(\tilde{\mathbf{x}} - \mathbf{x})^T \Phi | V_f(\tilde{\mathbf{x}}, \mathbf{x}) \leq \alpha]$ is zero. Since \mathbf{x} has elliptic distribution along any direction $\mathbf{w} \in \mathcal{S}_\Phi^\perp$, $\mathbf{w}^T(\mathbf{x} - \mathbb{E}\mathbf{x})$ and $-\mathbf{w}^T(\mathbf{x} - \mathbb{E}\mathbf{x})$ have the same distribution. Moreover, for any $\mathbf{w} \in \mathcal{S}_\Phi^\perp$, $\mathbf{w}^T(\tilde{\mathbf{x}} - \mathbf{x})$ is independent from the event $V_f(\tilde{\mathbf{x}}, \mathbf{x}) \leq \alpha$. Then

$$\mathbb{E} [\Psi^T(\tilde{\mathbf{x}} - \mathbf{x})(\tilde{\mathbf{x}} - \mathbf{x})^T \Phi | V_f(\tilde{\mathbf{x}}, \mathbf{x}) \leq \alpha] = -\mathbb{E} [\Psi^T(\tilde{\mathbf{x}} - \mathbf{x})(\tilde{\mathbf{x}} - \mathbf{x})^T \Phi | V_f(\tilde{\mathbf{x}}, \mathbf{x}) \leq \alpha] = \mathbf{0}.$$

Similarly, we have $\mathbb{E} [\Phi^T(\tilde{\mathbf{x}} - \mathbf{x})(\tilde{\mathbf{x}} - \mathbf{x})^T \Psi | V_f(\tilde{\mathbf{x}}, \mathbf{x}) \leq \alpha] = \mathbf{0}$. Let

$$\begin{aligned} G_1(\alpha) &= \mathbb{E} [\Phi^T(\tilde{\mathbf{x}} - \mathbf{x})(\tilde{\mathbf{x}} - \mathbf{x})^T \Phi | V(\tilde{\mathbf{x}}, \mathbf{x}) \leq \alpha] \in \mathbb{R}^{d \times d} \\ G_2(\alpha) &= \mathbb{E} [\Psi^T(\tilde{\mathbf{x}} - \mathbf{x})(\tilde{\mathbf{x}} - \mathbf{x})^T \Psi | V(\tilde{\mathbf{x}}, \mathbf{x}) \leq \alpha] \in \mathbb{R}^{(D-d) \times (D-d)}. \end{aligned}$$

and then the covariance matrix $G(\alpha)$ can be written as

$$G(\alpha) = \Phi G_1(\alpha) \Phi^T + \Psi G_2(\alpha) \Psi^T.$$

Let $\hat{\lambda}_1, \dots, \hat{\lambda}_d$ be the eigenvalues of $G_1(\alpha)$ and $\mathbf{z}_1, \dots, \mathbf{z}_d$ be the associated orthonormal eigenvectors, and let $\tilde{\lambda}_1, \dots, \tilde{\lambda}_{D-d}$ be the eigenvalues of $G_2(\alpha)$ and $\tilde{\mathbf{z}}_1, \dots, \tilde{\mathbf{z}}_{D-d}$ be the associated orthonormal eigenvectors. Then the eigenvalues of $G(\alpha)$ are $\hat{\lambda}_1, \dots, \hat{\lambda}_d, \tilde{\lambda}_1, \dots, \tilde{\lambda}_{D-d}$ and the associated eigenvectors are $\Phi \mathbf{z}_1, \dots, \Phi \mathbf{z}_d, \Psi \tilde{\mathbf{z}}_1, \dots, \Psi \tilde{\mathbf{z}}_{D-d}$ since

$$\begin{aligned} G(\alpha) \Phi \mathbf{z}_j &= \Phi G_1(\alpha) \Phi^T \Phi \mathbf{z}_j = \hat{\lambda}_j \Phi \mathbf{z}_j, j = 1, \dots, d, \\ G(\alpha) \Psi \tilde{\mathbf{z}}_k &= \Psi G_2(\alpha) \Psi^T \Psi \tilde{\mathbf{z}}_k = \tilde{\lambda}_k \Psi \tilde{\mathbf{z}}_k, k = 1, \dots, D - d. \end{aligned}$$

The eigenvalues satisfy

$$\begin{aligned} \hat{\lambda}_j &= (\Phi \mathbf{z}_j)^T G_1(\alpha) \Phi \mathbf{z}_j \\ &= \mathbf{z}_j^T \Phi^T \Phi \mathbb{E} [\Phi^T(\tilde{\mathbf{x}} - \mathbf{x})(\tilde{\mathbf{x}} - \mathbf{x})^T \Phi | V(\tilde{\mathbf{x}}, \mathbf{x}) \leq \alpha] \Phi^T \Phi \mathbf{z}_j \\ &= \mathbb{E} [\mathbf{z}_j^T \Phi^T(\tilde{\mathbf{x}} - \mathbf{x})(\tilde{\mathbf{x}} - \mathbf{x})^T \Phi \mathbf{z}_j | V(\tilde{\mathbf{x}}, \mathbf{x}) \leq \alpha] \\ &= \text{var} [(\Phi \mathbf{z}_j)^T(\tilde{\mathbf{x}} - \mathbf{x}) | V(\tilde{\mathbf{x}}, \mathbf{x}) \leq \alpha], j = 1, \dots, d; \\ \tilde{\lambda}_k &= \text{var} [(\Psi \tilde{\mathbf{z}}_k)^T(\tilde{\mathbf{x}} - \mathbf{x}) | V(\tilde{\mathbf{x}}, \mathbf{x}) \leq \alpha], k = 1, \dots, D - d. \end{aligned}$$

By Assumption 1, $\hat{\lambda}_j \leq \phi(\alpha), j = 1, \dots, d$ and $\tilde{\lambda}_k \geq C_0, k = 1, \dots, D - d$. □

B Proof of Lemma 2

Lemma 9 (Matrix Bernstein inequality [36]). *Let S_1, \dots, S_n be independent random matrices of size $D \times D$. Assume that each matrix has a bounded deviation from its mean:*

$$\|S_k - \mathbb{E}S_k\| \leq C \text{ for each } k = 1, \dots, n.$$

Form the sum $S = \sum_{k=1}^n S_k$, and introduce a variance parameter

$$\sigma_S^2 = \max \left\{ \|\mathbb{E}[(S - \mathbb{E}S)(S - \mathbb{E}S)^T]\|, \|\mathbb{E}[(S - \mathbb{E}S)^T(S - \mathbb{E}S)]\| \right\}.$$

Then

$$\mathbb{P}(\|S - \mathbb{E}S\| \geq t) \leq 2D \exp\left(\frac{-t^2/2}{\sigma_S^2 + Ct/3}\right) \text{ for all } t \geq 0,$$

and

$$\mathbb{E}(\|S - \mathbb{E}(S)\|) \leq \sqrt{2\sigma_S^2 \log(2D)} + \frac{1}{3}C \log(2D).$$

Lemma 2 is proved through the Matrix Bernstein inequality above.

Proof of Lemma 2. Denote the (i, j) pair in the sum of $\bar{G}(\alpha)$ as $(i_k, j_k), k = 1, 2, \dots, \bar{n}_\alpha$. For every k , $\mathbb{E}(\mathbf{x}_{i_k} - \mathbf{x}_{j_k})(\mathbf{x}_{i_k} - \mathbf{x}_{j_k})^T = G(\alpha)$ and then let

$$S = \bar{G}(\alpha) - G(\alpha) = \sum_{k=1}^{\bar{n}_\alpha} S_k, \text{ where } S_k = \frac{1}{\bar{n}_\alpha} [(\mathbf{x}_{i_k} - \mathbf{x}_{j_k})(\mathbf{x}_{i_k} - \mathbf{x}_{j_k})^T - G(\alpha)].$$

Notice that $\mathbb{E}(S_k) = 0$, and $\|S_k\| \leq \frac{8B^2}{\bar{n}_\alpha}$ for $k = 1, 2, \dots, \bar{n}_\alpha$. The variance parameter can be estimated from

$$\begin{aligned} \mathbb{E}S_k^2 &= \frac{1}{\bar{n}_\alpha^2} \mathbb{E} \left(\|(\mathbf{x}_{i_k} - \mathbf{x}_{j_k})\|_2^2 (\mathbf{x}_{i_k} - \mathbf{x}_{j_k})(\mathbf{x}_{i_k} - \mathbf{x}_{j_k})^T - (\mathbf{x}_{i_k} - \mathbf{x}_{j_k})(\mathbf{x}_{i_k} - \mathbf{x}_{j_k})^T G(\alpha) \right. \\ &\quad \left. - G(\alpha)(\mathbf{x}_{i_k} - \mathbf{x}_{j_k})(\mathbf{x}_{i_k} - \mathbf{x}_{j_k})^T + G^2(\alpha) \right) \\ &\preceq \frac{1}{\bar{n}_\alpha^2} (4B^2 \mathbb{E}[(\mathbf{x}_{i_k} - \mathbf{x}_{j_k})(\mathbf{x}_{i_k} - \mathbf{x}_{j_k})^T] - G^2(\alpha)) \preceq \frac{4B^2}{\bar{n}_\alpha^2} G(\alpha), \end{aligned}$$

such that

$$\sigma_S^2 = \mathbb{E}S^2 = \mathbb{E} \left(\sum_{k=1}^{\bar{n}_\alpha} S_k \right)^2 = \mathbb{E} \left(\sum_{k=1}^{\bar{n}_\alpha} S_k^2 \right) \leq \frac{4B^2}{\bar{n}_\alpha} \|G(\alpha)\| \leq \frac{16B^4}{\bar{n}_\alpha},$$

where the last inequality holds as $\|G(\alpha)\| \leq 4B^2$. Applying the matrix Bernstein inequality in Lemma 9 yields

$$\mathbb{P}(\|\bar{G}(\alpha) - G(\alpha)\| \geq t) \leq 2D \exp\left(\frac{-3t^2\bar{n}_\alpha}{16B^2(6B^2 + t)}\right),$$

$$\begin{aligned} \mathbb{E}(\|\bar{G}(\alpha) - G(\alpha)\|) &\leq \sqrt{\frac{32B^4 \log(2D)}{\bar{n}_\alpha}} + \frac{8B^2 \log(2D)}{3\bar{n}_\alpha} \\ &\leq 4B^2 \left(\sqrt{\frac{2 \log(2D)}{\bar{n}_\alpha}} + \frac{2 \log(2D)}{3\bar{n}_\alpha} \right) \\ &\leq 8B^2 \sqrt{\frac{2 \log(2D)}{\bar{n}_\alpha}} \text{ when } \bar{n}_\alpha \geq \frac{2 \log(2D)}{3}. \end{aligned}$$

□

C Proof of Lemma 3

Recall that $\widehat{G}(\alpha, r)$ sums over independent matrices $(\mathbf{x}_i - \mathbf{x}_j)(\mathbf{x}_i - \mathbf{x}_j)^T$ satisfying $\widehat{V}_y(\mathbf{x}_i, \mathbf{x}_j, r) \leq \alpha$, while $\bar{G}(\alpha + \alpha_0 + 3\sigma^2)$ sums over independent matrices $(\mathbf{x}_i - \mathbf{x}_j)(\mathbf{x}_i - \mathbf{x}_j)^T$ satisfying $V_f(\mathbf{x}_i, \mathbf{x}_j) \leq \alpha + \alpha_0 + 3\sigma^2$. To prove $\widehat{G}(\alpha, r) = \bar{G}(\alpha + \alpha_0 + 3\sigma^2)$ with high probability, it is sufficient to show that $\widehat{V}_y(\mathbf{x}_i, \mathbf{x}_j, r) \leq \alpha$ implies $V_f(\mathbf{x}_i, \mathbf{x}_j) \leq \alpha + \alpha_0 + 3\sigma^2$ with high probability. We express

$$\begin{aligned} V_f(\mathbf{x}_i, \mathbf{x}_j) - \widehat{V}_y(\mathbf{x}_i, \mathbf{x}_j, r) &= V_f(\mathbf{x}_i, \mathbf{x}_j) - V_f(\mathbf{x}_i, \mathbf{x}_j, r) \\ &\quad + V_f(\mathbf{x}_i, \mathbf{x}_j, r) - V_y(\mathbf{x}_i, \mathbf{x}_j, r) + V_y(\mathbf{x}_i, \mathbf{x}_j, r) - \widehat{V}_y(\mathbf{x}_i, \mathbf{x}_j, r). \end{aligned}$$

where $V_f(\mathbf{x}_i, \mathbf{x}_j, r) = \text{var}(f(\mathbf{x}) | \mathbf{x} \in T_{ij}(r))$ and thus

$$\begin{aligned} |V_f(\mathbf{x}_i, \mathbf{x}_j) - \widehat{V}_y(\mathbf{x}_i, \mathbf{x}_j, r)| &\leq \underbrace{|V_f(\mathbf{x}_i, \mathbf{x}_j) - V_f(\mathbf{x}_i, \mathbf{x}_j, r)|}_{\text{I}} \\ &\quad + \underbrace{|V_f(\mathbf{x}_i, \mathbf{x}_j, r) - V_y(\mathbf{x}_i, \mathbf{x}_j, r)|}_{\text{II}} + \underbrace{|V_y(\mathbf{x}_i, \mathbf{x}_j, r) - \widehat{V}_y(\mathbf{x}_i, \mathbf{x}_j, r)|}_{\text{III}}. \end{aligned} \tag{S.1}$$

The second term satisfies $\text{II} \leq \sigma^2$ since it captures the variance of the bounded noise in $[-\sigma, \sigma]$. The first term represents the difference between the variance of f over the segment between \mathbf{x}_i and \mathbf{x}_j , and the variance of f in the tube with radius r enclosing this segment. Under the condition that g is Lipschitz, it scales linearly with respect to the tube radius r . An upper bound of I is given below:

Lemma 10. *Assume Assumption 2(i) and 3, and f is defined as (1). For every $\mathbf{x}_i, \mathbf{x}_j \in \mathbb{R}^D$ and sufficiently small r ,*

$$|V_f(\mathbf{x}_i, \mathbf{x}_j) - V_f(\mathbf{x}_i, \mathbf{x}_j, r)| \leq 10L_g^2 Br. \tag{S.2}$$

Proof of Lemma 10. Let \bar{f}_ℓ be the mean of $f(\mathbf{x})$ on $\ell(\mathbf{x}_i, \mathbf{x}_j)$ and \bar{f}_{ij} be the mean of $f(\mathbf{x})$ on $T_{ij}(r)$. We first prove the error bound between \bar{f}_ℓ and \bar{f}_{ij} . For simplicity, we denote $\ell(\mathbf{x}_i, \mathbf{x}_j)$ by ℓ . We parameterize ℓ by t for $0 \leq t \leq 1$ and use $\mathbf{r}(t)$ to denote a point on ℓ such that $\mathbf{r}(0) = \mathbf{x}_i$ and $\mathbf{r}(1) = \mathbf{x}_j$. Let $\mathbb{S}(t)$ be the disk centered at $\mathbf{r}(t)$ of radius r on the hyperplane of dimension $D - 1$ which is perpendicular to ℓ . Let ρ^t be a measure on $[0, 1]$ such that, for any $\mathbf{r}(t) \in \ell$, $\rho^t(dt) = \lim_{r \rightarrow 0} \frac{\rho(T(\mathbf{r}(t), \mathbf{r}(t+dt), r))}{\rho(T(\mathbf{r}(0), \mathbf{r}(1), r))}$, where $T(\mathbf{r}(t), \mathbf{r}(t+dt), r)$ is the tube enclosing $\ell(\mathbf{r}(t), \mathbf{r}(t+dt))$ with radius r . We can express

$$\bar{f}_\ell = \int_0^1 f(\mathbf{r}(t)) \rho^t(dt) = \lim_{r \rightarrow 0} \frac{1}{\rho(T_{ij}(r))} \int_0^1 \int_{\mathbb{S}(t)} f(\mathbf{r}(t)) \rho(\mathbb{S}(t)) dt$$

and

$$\bar{f}_{ij} = \frac{1}{\rho(T_{ij}(r))} \int_{T_{ij}(r)} f(\mathbf{x}) \rho(d\mathbf{x}) = \frac{1}{\rho(T_{ij}(r))} \int_0^1 \int_{\mathbb{S}(t)} f(\mathbf{x}) \rho(\mathbb{S}(t)) dt.$$

When $r \rightarrow 0$,

$$|\bar{f}_\ell - \bar{f}_{ij}| = \frac{1}{\rho(T_{ij}(r))} \left| \int_0^1 \int_{\mathbb{S}(t)} [f(\mathbf{r}(t)) - f(\mathbf{x})] \rho(\mathbb{S}(t)) dt \right| \leq rL_g.$$

We next derive the error bound between $V_f(\mathbf{x}_i, \mathbf{x}_j)$ and $V_f(\mathbf{x}_i, \mathbf{x}_j, r)$ when $r \rightarrow 0$:

$$\begin{aligned}
& |V_f(\mathbf{x}_i, \mathbf{x}_j) - V_f(\mathbf{x}_i, \mathbf{x}_j, r)| \\
&= \left| \frac{1}{\rho(T_{ij}(r))} \int_0^1 \int_{\mathbb{S}(t)} (f(\mathbf{r}(t)) - \bar{f}_\ell)^2 \rho(\mathbb{S}(t)) dt - \frac{1}{\rho(T_{ij}(r))} \int_0^1 \int_{\mathbb{S}(t)} (f(\mathbf{x})) - \bar{f}_{ij})^2 \rho(\mathbb{S}(t)) dt \right| \\
&= \frac{1}{\rho(T_{ij}(r))} \int_0^1 \int_{\mathbb{S}(t)} |(f(\mathbf{r}(t)) - \bar{f}_\ell)^2 - (f(\mathbf{x}) - \bar{f}_{ij})^2| \rho(\mathbb{S}(t)) dt \\
&= \frac{1}{\rho(T_{ij}(r))} \int_0^1 \int_{\mathbb{S}(t)} |(f(\mathbf{r}(t)) - \bar{f}_\ell + f(\mathbf{x}) - \bar{f}_{ij})(f(\mathbf{r}(t)) - f(\mathbf{x}) + \bar{f}_{ij} - \bar{f}_\ell)| \rho(\mathbb{S}(t)) dt \\
&\leq \frac{1}{\rho(T_{ij}(r))} \int_0^1 \int_{\mathbb{S}(t)} |(f(\mathbf{r}(t)) - \bar{f}_\ell + f(\mathbf{x}) - \bar{f}_{ij})| \cdot 2r L_g \rho(\mathbb{S}(t)) dt.
\end{aligned}$$

On the other hand, for any $\mathbf{r}(t) \in \ell$,

$$|f(\mathbf{r}(t)) - \bar{f}_\ell| \leq L_g \|\mathbf{x}_i - \mathbf{x}_j\| \leq 2L_g B.$$

Similarly, for any $\mathbf{x} \in T_{ij}(r)$

$$|f(\mathbf{x}) - \bar{f}_{ij}| \leq L_g \sup_{\mathbf{z}, \mathbf{w} \in T_{ij}(r)} \|\mathbf{z} - \mathbf{w}\| = L_g \sqrt{\|\mathbf{x}_i - \mathbf{x}_j\|^2 + 4r^2} \leq 3L_g B$$

when $4r^2 \leq 5B^2$. In summary,

$$|V_f(\mathbf{x}_i, \mathbf{x}_j) - V_f(\mathbf{x}_i, \mathbf{x}_j, r)| \leq 10L_g^2 B r.$$

□

The term III captures the difference between the population variance of y in the tube $T_{ij}(r)$ and its empirical counterpart. We expect it to be small if there are sufficient amount of points in $T_{ij}(r)$. The following lemma gives an estimate on the difference between the population variance of a bounded random variable and its empirical counterpart.

Lemma 11. *Let s be a random variable in $[m - A, m + A]$ for some $m \in \mathbb{R}$ and $A > 0$. Suppose $\{s_i\}_{i=1}^n$ are independent copies of s . Denote the empirical variance by $\hat{V}(s) = \frac{1}{n-1} \sum_{i=1}^n (s_i - \bar{s})^2$ where $\bar{s} = (s_1 + \dots + s_n)/n$. Then*

$$\mathbb{P} \left(|\hat{V}(s) - \mathbb{E}\hat{V}(s)| \geq t \right) \leq 2e^{-\frac{nt^2}{16A^4}} \quad \text{for any } t > 0.$$

Lemma 11 is a consequence of U-statistics [19] applied on $\hat{V}(s)$. We next derive an estimate of III in (S.1) based on Lemma 11.

Lemma 12. *Let $\{\mathbf{x}_i\}_{i=1}^n$ be i.i.d. samples from the probability measure ρ , and $\{y_i\}_{i=1}^n$ be sampled according to the model in (1), under Assumption 2(i) (ii), 3 and 4. Let $\nu > 0$ and set*

$$\alpha_0 = \max \left\{ C_2 \left(\frac{\log n}{n} \right)^{\frac{1}{D}}, C_3 \left(\frac{\log n}{n} \right)^{\frac{1}{D+2}} \right\} \quad \text{and } r = C_1 \alpha_0 \quad (\text{S.3})$$

with some $C_1 \leq 1/(8L_g^2)$, $C_2 = [56\nu L_g^2 / (3c_0 C_1^{D-1})]^{\frac{1}{D}}$, $C_3 = [256\nu(M + \sigma)^4 L_g^2 / (c_0 C_1^{D-1})]^{\frac{1}{D+2}}$. Then

$$\mathbb{P} \left\{ |V_y(\mathbf{x}_i, \mathbf{x}_j, r) - \hat{V}_y(\mathbf{x}_i, \mathbf{x}_j, r)| \leq \frac{\alpha_0}{2} + 2\sigma^2 \right\} \geq 1 - 4n^{-\nu}.$$

Proof of Lemma 12. We set $\eta = \alpha_0/(2L_g^2)$, and consider the tube $T_{ij}(r)$ with $\|\mathbf{x}_i - \mathbf{x}_j\| > \eta$ and $\|\mathbf{x}_i - \mathbf{x}_j\| \leq \eta$ as separate cases.

Case I when $\|\mathbf{x}_i - \mathbf{x}_j\| \leq \eta$: When $\|\mathbf{x}_i - \mathbf{x}_j\| \leq \eta$, we expect $V_y(\mathbf{x}_i, \mathbf{x}_j, r)$ to be small since $f(\mathbf{x})$ has a small variation within $T_{ij}(r)$. Let $\mathbf{z} = (\mathbf{x}_i + \mathbf{x}_j)/2$. For any $\mathbf{x} \in T_{ij}(r)$, $|f(\mathbf{x}) - f(\mathbf{z})| \leq L_g \sqrt{(\eta/2)^2 + r^2}$. Hence,

$$\begin{aligned} |V_y(\mathbf{x}_i, \mathbf{x}_j, r) - \widehat{V}_y(\mathbf{x}_i, \mathbf{x}_j, r)| &\leq \max(V_y(\mathbf{x}_i, \mathbf{x}_j, r), \widehat{V}_y(\mathbf{x}_i, \mathbf{x}_j, r)) \\ &\leq 2(L_g^2[(\eta/2)^2 + r^2] + \sigma^2) \leq \alpha_0/2 + 2\sigma^2 \end{aligned}$$

where the last inequality holds as long as $\eta^2 \leq \alpha_0/(2L_g^2)$ and $r^2 \leq \alpha_0/(8L_g^2)$. By (S.3), α_0 is small when n is sufficiently large. These conditions are guaranteed as $\eta^2 < \eta = \alpha_0/(2L_g^2)$ and $r^2 < r \leq \alpha_0/(8L_g^2)$ when n is sufficiently large.

Case II when $\|\mathbf{x}_i - \mathbf{x}_j\| > \eta$: When $\|\mathbf{x}_i - \mathbf{x}_j\| > \eta$, there are sufficient points in $T_{ij}(r)$ so that $\widehat{V}_y(\mathbf{x}_i, \mathbf{x}_j, r)$ is concentrated on $V_y(\mathbf{x}_i, \mathbf{x}_j, r)$. Let $\rho(T_{ij}(r))$ be the measure of the tube $T_{ij}(r)$, which satisfies $\rho(T_{ij}(r)) \geq c_0 r^{D-1} \eta$ by (7). Let $n_{ij}(r)$ be the number of points in $T_{ij}(r)$ and then $\widehat{\rho}(T_{ij}(r)) = n_{ij}(r)/n$ is the empirical measure of $T_{ij}(r)$. By [29, Lemma 29], we have the following concentration of measure:

$$\mathbb{P} \left\{ |\widehat{\rho}(T_{ij}(r)) - \rho(T_{ij}(r))| \geq \frac{1}{2} \rho(T_{ij}(r)) \right\} \leq 2e^{-\frac{3}{28} n \rho(T_{ij}(r))} \leq 2e^{-\frac{3}{28} c_0 n r^{D-1} \eta} \quad (\text{S.4})$$

On the condition of the event $|\widehat{\rho}(T_{ij}(r)) - \rho(T_{ij}(r))| \leq \frac{1}{2} \rho(T_{ij}(r))$, we have $\widehat{\rho}(T_{ij}(r)) \geq \frac{1}{2} \rho(T_{ij}(r))$, which implies $n_{ij}(r) \geq \frac{1}{2} c_0 n r^{D-1} \eta$. By Lemma 11, $\widehat{V}_y(\mathbf{x}_i, \mathbf{x}_j, r)$ is concentrated on $V_y(\mathbf{x}_i, \mathbf{x}_j, r)$ with high probability:

$$\mathbb{P} \left\{ |V_y(\mathbf{x}_i, \mathbf{x}_j, r) - \widehat{V}_y(\mathbf{x}_i, \mathbf{x}_j, r)| \geq t \right\} \leq 2e^{-\frac{n_{ij}(r)t^2}{16(M+\sigma)^4}}, \forall t > 0.$$

Setting $t = \frac{1}{2} \alpha_0$ gives rise to

$$\begin{aligned} \mathbb{P} \left\{ |V_y(\mathbf{x}_i, \mathbf{x}_j, r) - \widehat{V}_y(\mathbf{x}_i, \mathbf{x}_j, r)| \geq \frac{1}{2} \alpha_0 \mid |\widehat{\rho}(T_{ij}(r)) - \rho(T_{ij}(r))| \leq \frac{1}{2} \rho(T_{ij}(r)) \right\} \\ \leq 2e^{-\frac{n_{ij}(r)\alpha_0^2}{64(M+\sigma)^4}} \leq e^{-\frac{c_0 n r^{D-1} \eta \alpha_0^2}{128(M+\sigma)^4}} \end{aligned} \quad (\text{S.5})$$

Combining (S.4) and (S.5) yields

$$\begin{aligned} \mathbb{P} \left\{ |V_y(\mathbf{x}_i, \mathbf{x}_j, r) - \widehat{V}_y(\mathbf{x}_i, \mathbf{x}_j, r)| \geq \frac{1}{2} \alpha_0 \right\} &\leq \mathbb{P} \left\{ |\widehat{\rho}(T_{ij}(r)) - \rho(T_{ij}(r))| \geq \frac{1}{2} \rho(T_{ij}(r)) \right\} \\ &+ \mathbb{P} \left\{ |V_y(\mathbf{x}_i, \mathbf{x}_j, r) - \widehat{V}_y(\mathbf{x}_i, \mathbf{x}_j, r)| \geq \frac{1}{2} \alpha_0 \mid |\widehat{\rho}(T_{ij}(r)) - \rho(T_{ij}(r))| \leq \frac{1}{2} \rho(T_{ij}(r)) \right\} \\ &\leq 2e^{-\frac{3}{28} c_0 n r^{D-1} \eta} + 2e^{-\frac{c_0 n r^{D-1} \eta \alpha_0^2}{128(M+\sigma)^4}} \leq 2e^{-\frac{3c_0 C_1^{D-1} n \alpha_0^D}{56L_g^2}} + 2e^{-\frac{c_0 C_1^{D-1} n \alpha_0^{D+2}}{256(M+\sigma)^4 L_g^2}}. \end{aligned}$$

When α_0 is chosen according to (S.3), one obtains

$$\mathbb{P} \left\{ |V_y(\mathbf{x}_i, \mathbf{x}_j, r) - \widehat{V}_y(\mathbf{x}_i, \mathbf{x}_j, r)| \geq \frac{1}{2} \alpha_0 \right\} \leq 4n^{-\nu}.$$

□

Combining Lemma 10 and Lemma 12, we obtain the following estimate of $|V_f(\mathbf{x}_i, \mathbf{x}_j) - \widehat{V}_y(\mathbf{x}_i, \mathbf{x}_j, r)|$:

Lemma 13. *Let $\{\mathbf{x}_i\}_{i=1}^n$ be i.i.d. samples from the probability measure ρ , and $\{y_i\}_{i=1}^n$ be sampled according to the model in (1), under Assume Assumption 2(i) (ii), 3 and 4. Let $\nu > 0$ and set α_0 and r as (S.3) with $C_1 = (4L_g^2 \max(5B, 2))^{-1}$. Then*

$$\mathbb{P} \left(|V_f(\mathbf{x}_i, \mathbf{x}_j) - \widehat{V}_y(\mathbf{x}_i, \mathbf{x}_j, r)| \leq \alpha_0 + 3\sigma^2 \right) \geq 1 - 4n^{-\nu}. \quad (\text{S.6})$$

Proof of Lemma 13. The proof is based on a combination of Lemma 10 and Lemma 12. In (S.1), we have

$$\begin{aligned} \text{I} &\leq \frac{\alpha_0}{2} \text{ if } r \leq \frac{\alpha_0}{20L_g^2 B} \text{ from Lemma 10,} \\ \text{II} &\leq \sigma^2, \\ \text{III} &\leq \frac{\alpha_0}{2} + 2\sigma^2 \text{ with probability no less than } 1 - 4n^{-\nu}, \end{aligned}$$

which implies (S.6). □

Lemma 13 gives an estimate on $|V_f(\mathbf{x}_i, \mathbf{x}_j) - \widehat{V}_y(\mathbf{x}_i, \mathbf{x}_j, r)|$ for an (i, j) pair. We next derive a union bound to show that if n is large enough, then with high probability, every $V_f(\mathbf{x}_i, \mathbf{x}_j)$ is small for all the (i, j) pairs satisfying $\mathcal{A}(i, j) = 1$.

Lemma 14. *Let $\{\mathbf{x}_i\}_{i=1}^n$ be i.i.d. samples from the probability measure ρ , and $\{y_i\}_{i=1}^n$ be sampled according to the model in (1), under Assumption 2(i) (ii), 3 and 4. Let $\nu > 0$ and set α_0, r as (S.3). Index the output pairs $\{(\mathbf{x}_i, \mathbf{x}_j) | \mathcal{A}(i, j) = 1\}$ by Algorithm 1 as $\{(\mathbf{x}_{i_k}, \mathbf{x}_{j_k})\}_{k=1}^{\widehat{n}_\alpha}$. Then for any $\alpha > 0$,*

$$\mathbb{P} \left(\bigcap_{k=1}^{\widehat{n}_\alpha} [V_f(\mathbf{x}_{i_k}, \mathbf{x}_{j_k}) \leq \alpha + \alpha_0 + 3\sigma^2] \right) \geq 1 - 4\widehat{n}_\alpha n^{-\nu}.$$

Proof of Lemma 14. Lemma 13 implies that, for any $\alpha > 0$,

$$\mathbb{P} (V_f(\mathbf{x}_{i_k}, \mathbf{x}_{j_k}) > \alpha + \alpha_0 + 3\sigma^2) \leq 4n^{-\nu}.$$

Then

$$\begin{aligned} \mathbb{P} \left(\bigcap_{k=1}^{\widehat{n}_\alpha} [V_f(\mathbf{x}_{i_k}, \mathbf{x}_{j_k}) \leq \alpha + \alpha_0 + 3\sigma^2] \right) &= 1 - \mathbb{P} \left(\bigcup_{k=1}^{\widehat{n}_\alpha} [V_f(\mathbf{x}_{i_k}, \mathbf{x}_{j_k}) > \alpha + \alpha_0 + 3\sigma^2] \right) \\ &\geq 1 - \sum_{k=1}^{\widehat{n}_\alpha} \mathbb{P} (V_f(\mathbf{x}_{i_k}, \mathbf{x}_{j_k}) > \alpha + \alpha_0 + 3\sigma^2) \geq 1 - 4\widehat{n}_\alpha n^{-\nu}. \end{aligned}$$

□

Proof of Lemma 3. $\widehat{G}(\alpha, r)$ sums over \widehat{n}_α pairs of $(\mathbf{x}_i, \mathbf{x}_j)$ such that $\widehat{V}_y(\mathbf{x}_i, \mathbf{x}_j, r) \leq \alpha$. By Lemma 14, all of these \widehat{n}_α pairs of $(\mathbf{x}_i, \mathbf{x}_j)$ satisfies $V_f(\mathbf{x}_i, \mathbf{x}_j) \leq \alpha + \alpha_0 + 3\sigma^2$ with probability no less than $1 - 4\widehat{n}_\alpha n^{-\nu}$. □

D Proof of Lemma 4

To prove Lemma 4, we need the following Lemma:

Lemma 15. Suppose f is defined as (1), with the function g satisfying Assumption 3. For any two points $\mathbf{x}_i, \mathbf{x}_j \in \mathbb{R}^D$, $V_f(\mathbf{x}_i, \mathbf{x}_j) \leq L_g^2 \|\Phi^T \mathbf{x}_i - \Phi^T \mathbf{x}_j\|^2$.

Proof. For any $\mathbf{x} = (1-t)\mathbf{x}_i + t\mathbf{x}_j, t \in [0, 1]$, we have

$$\begin{aligned} |f(\mathbf{x}) - f(\mathbf{x}_i)| &= |g(\Phi^T \mathbf{x}) - g(\Phi^T \mathbf{x}_i)| \\ &\leq L_g \|\Phi^T [(1-t)\mathbf{x}_i + t\mathbf{x}_j] - \Phi^T \mathbf{x}_i\| \\ &= L_g \|t(\Phi^T \mathbf{x}_j - \Phi^T \mathbf{x}_i)\| \leq L_g \|\Phi^T \mathbf{x}_i - \Phi^T \mathbf{x}_j\|. \end{aligned}$$

Therefore, $V_f(\mathbf{x}_i, \mathbf{x}_j) = \text{var}(f(\mathbf{x}) | \mathbf{x} = (1-t)\mathbf{x}_i + t\mathbf{x}_j, t \in [0, 1]) \leq L_g^2 \|\Phi^T \mathbf{x}_i - \Phi^T \mathbf{x}_j\|^2$. \square

Proof of Lemma 4. In Algorithm 1, we say two points $\mathbf{x}_i, \mathbf{x}_j$ are connected if Algorithm 1 outputs $\mathcal{A}(\mathbf{x}_i, \mathbf{x}_j) = 1$. Algorithm 1 guarantees that if \mathbf{x}_i and \mathbf{x}_j are connected, they can not be connected with any other points, so that the connected pairs are independent from each other. As a consequence, \hat{n}_α is upper bounded by $n/2$.

To prove the lower bound of \hat{n}_α , we first discretize the domain $[-B, B]^d$ into small cubes along each direction with grid spacing $h = 2B(\log n/n)^{\frac{1}{2D}}$. Denote the d -dimensional cube with side length h as $\tilde{\Omega}_k, k = 1, \dots, N$, and then $N \leq (2B/h)^d = (n/\log n)^{\frac{d}{2D}}$. Define N prisms in \mathbb{R}^D as

$$\Omega_k = \{\mathbf{x} \in \mathbb{R}^D : \Phi^T \mathbf{x} \in \tilde{\Omega}_k\}, \quad k = 1, \dots, N.$$

For any Ω_k and any $\mathbf{x}_i, \mathbf{x}_j \in \Omega_k$, we next show $\hat{V}_y(\mathbf{x}_i, \mathbf{x}_j, r) \leq \alpha$ with high probability. If $\mathbf{x}_i, \mathbf{x}_j \in \Omega_k$, $\|\Phi^T \mathbf{x}_i - \Phi^T \mathbf{x}_j\| \leq \sqrt{d}h$ and by Lemma 15, $V_f(\mathbf{x}_i, \mathbf{x}_j) \leq dL_g^2 h^2 = 4dL_g^2 B^2 (\log n/n)^{\frac{1}{D}}$. According to Lemma 13, $\mathbb{P}(|V_f(\mathbf{x}_i, \mathbf{x}_j) - \hat{V}_y(\mathbf{x}_i, \mathbf{x}_j, r)| \leq \alpha_0 + 3\sigma^2) \geq 1 - 4n^{-\nu}$. Therefore, for any $\mathbf{x}_i, \mathbf{x}_j \in \Omega_k$, we have

$$\mathbb{P}\left\{\hat{V}_y(\mathbf{x}_i, \mathbf{x}_j, r) > 4dL_g^2 B^2 \left(\frac{\log n}{n}\right)^{\frac{1}{D}} + \alpha_0 + 3\sigma^2\right\} \leq 4n^{-\nu}.$$

Denote $\#\Omega_k = \#\{\mathbf{x}_i : \mathbf{x}_i \in \Omega_k\}$. Applying a union bound gives

$$\begin{aligned} &\mathbb{P}\left\{\exists \Omega_k \text{ such that } \exists \mathbf{x}_i, \mathbf{x}_j \in \Omega_k : \hat{V}_y(\mathbf{x}_i, \mathbf{x}_j, r) > 4dL_g^2 B^2 \left(\frac{\log n}{n}\right)^{\frac{1}{D}} + \alpha_0 + 3\sigma^2\right\} \\ &\leq \sum_k \mathbb{P}\left\{\exists \mathbf{x}_i, \mathbf{x}_j \in \Omega_k : \hat{V}_y(\mathbf{x}_i, \mathbf{x}_j, r) > 4dL_g^2 B^2 \left(\frac{\log n}{n}\right)^{\frac{1}{D}} + \alpha_0 + 3\sigma^2\right\} \\ &\leq \sum_k \binom{\#\Omega_k}{2} 4n^{-\nu} \leq \sum_k 2(\#\Omega_k)^2 n^{-\nu} \leq 2 \left(\sum_k \#\Omega_k\right)^2 n^{-\nu} \leq 2n^{-(\nu-2)}. \end{aligned}$$

The equation above shows that, in all sets $\Omega_k, k = 1, \dots, N$, all pairs of points $\mathbf{x}_i, \mathbf{x}_j$ in each Ω_k satisfy $\hat{V}_y(\mathbf{x}_i, \mathbf{x}_j, r) \leq \alpha$ with probability no less than $1 - 2n^{-(\nu-2)}$.

In Algorithm 1, two points $\mathbf{x}_i, \mathbf{x}_j$ are likely to be connected if $\hat{V}_y(\mathbf{x}_i, \mathbf{x}_j, r) \leq \alpha$. Under the condition that in all the sets $\Omega_k, k = 1, \dots, N$, all pairs of points $\mathbf{x}_i, \mathbf{x}_j$ in each Ω_k

satisfy $\widehat{V}_y(\mathbf{x}_i, \mathbf{x}_j, r) \leq \alpha$, there is at most one point in each Ω_k that is not connected with other points in the output of Algorithm 1. Therefore, the number of connected pairs satisfies

$$\widehat{n}_\alpha \geq \frac{1}{2}(n - N) = \frac{1}{2} \left[n - \left(\frac{n}{\log n} \right)^{\frac{d}{2D}} \right] \geq \frac{n}{4}$$

if n is sufficiently large such that $2(n/\log n)^{\frac{d}{2D}} \leq n$. □

E Proof of Lemma 7

Proof of Lemma 7. $\mathbb{E}(X^2)$ can be computed by the following integral

$$\begin{aligned} \mathbb{E}(X^2) &= \int_0^{+\infty} t A e^{-\frac{at^2}{b+ct}} dt \\ &= \int_0^{+\infty} t \min(1, A e^{-\frac{at^2}{b+ct}}) dt \\ &\leq \int_0^{t_0} t dt + \int_{t_0}^{t_1} t A e^{-\frac{at^2}{2b}} dt + \int_{t_1}^{+\infty} t A e^{-\frac{at}{2c}} dt \\ &\leq \frac{1}{2} t_0^2 + \frac{Ab}{a} \left(e^{-\frac{at_0^2}{2b}} - e^{-\frac{at_1^2}{2b}} \right) + \frac{2c}{a} A e^{-\frac{at_1}{2c}} \left(t_1 + \frac{2c}{a} \right) \end{aligned}$$

where $A e^{-\frac{at_0^2}{2b}} = 1$, $b = ct_1$ such that $t_0^2 = (2b/a) \log A$ and $t_1 = b/c$. Plugging t_0 and t_1 to the equation above gives rise to

$$\begin{aligned} \mathbb{E}(X^2) &\leq \frac{b \log A}{a} + \frac{b}{a} - \frac{Ab}{a} e^{-\frac{ab}{2c^2}} + \frac{2Ab}{a} e^{-\frac{ab}{2c^2}} + \frac{4Ac^2}{a^2} e^{-\frac{ab}{2c^2}} \\ &= \frac{b}{a} (\log A + A e^{-\frac{ab}{2c^2}} + 1) + e^{-\frac{ab}{2c^2}} \frac{4Ac^2}{a^2} \\ &\leq \frac{b}{a} (\log A + A + 1) + \frac{4Ac^2}{a^2}. \end{aligned}$$
□

F Proof of Lemma 8

Lemma 8 is based Lemma 16 ([16, Lemma 11.1]) and Lemma 17 ([16, Theorem 11.3]) below, which are standard results in non-parametric statistics.

Lemma 16. [16, Lemma 11.1] Suppose $g : [-B, B]^d \rightarrow \mathbb{R}$ is (s, C_g) -smooth with $s = k + \beta$ for some $k \in \mathbb{N}_0$ and $\beta \in (0, 1]$. Let g_k be the Taylor polynomial of g at $\mathbf{a} \in [-B, B]^d$ of degree k . Then

$$|g(\mathbf{z}) - g_k(\mathbf{z})| \leq \frac{C_g d^{k/2} \|\mathbf{z} - \mathbf{a}\|^s}{k!},$$

for all \mathbf{z} near \mathbf{a} .

Proof of Lemma 16. We denote the multi-index $\alpha = (\alpha_1, \dots, \alpha_d)$ and let $\alpha! = \alpha_1! \cdots \alpha_d!$, $\mathbf{z}^\alpha = z_1^{\alpha_1} \cdots z_d^{\alpha_d}$ for $\mathbf{z} = (z_1, \dots, z_d)$. Denote the partial derivative $D^\alpha := \frac{\partial^{\alpha_1 + \dots + \alpha_d}}{\partial x_1^{\alpha_1} \cdots \partial x_d^{\alpha_d}}$. The Taylor expansion of g at \mathbf{a} gives

$$\begin{aligned} g(\mathbf{z}) - g_k(\mathbf{z}) &= g(\mathbf{z}) - g_{k-1}(\mathbf{z}) - \sum_{|\alpha|=k} \frac{D^\alpha g(\mathbf{a})(\mathbf{z} - \mathbf{a})^\alpha}{\alpha!} \\ &= \sum_{|\alpha|=k} \frac{k}{\alpha!} \left[\int_0^1 (1-t)^{k-1} D^\alpha g(\mathbf{a} + t(\mathbf{z} - \mathbf{a})) dt \right] (\mathbf{z} - \mathbf{a})^\alpha - \sum_{|\alpha|=k} \frac{(D^\alpha g)(\mathbf{a})(\mathbf{z} - \mathbf{a})^\alpha}{\alpha!} \\ &= \sum_{|\alpha|=k} \frac{(\mathbf{z} - \mathbf{a})^\alpha}{\alpha!} k \int_0^1 [(1-t)^{k-1} D^\alpha g(\mathbf{a} + t(\mathbf{z} - \mathbf{a})) - (1-t)^{k-1} D^\alpha g(\mathbf{a})] dt \\ &= \sum_{|\alpha|=k} \frac{(\mathbf{z} - \mathbf{a})^\alpha}{\alpha!} k \int_0^1 (1-t)^{k-1} [D^\alpha g(\mathbf{a} + t(\mathbf{z} - \mathbf{a})) - (D^\alpha g)(\mathbf{a})] dt. \end{aligned}$$

From this, and the assumption that g is (s, C_g) smooth, one obtains

$$\begin{aligned} |g(\mathbf{z}) - g_k(\mathbf{z})| &\leq \sum_{|\alpha|=k} \frac{|(\mathbf{z} - \mathbf{a})^\alpha|}{\alpha!} k \int_0^1 (1-t)^{k-1} C_g \|\mathbf{z} - \mathbf{a}\|^\beta dt \\ &= C_g \|\mathbf{z} - \mathbf{a}\|^\beta \sum_{|\alpha|=k} \frac{|(\mathbf{z} - \mathbf{a})^\alpha|}{\alpha!} = \frac{C_g \|\mathbf{z} - \mathbf{a}\|^\beta}{k!} \sum_{|\alpha|=k} \frac{k!}{\alpha!} |(\mathbf{z} - \mathbf{a})^\alpha| \\ &\text{by the multinomial theorem} \\ &= \frac{C_g \|\mathbf{z} - \mathbf{a}\|^\beta}{k!} \left(\sum_i |\mathbf{z}_i - \mathbf{a}_i| \right)^k \leq \frac{C_g \|\mathbf{z} - \mathbf{a}\|^\beta}{k!} \|\mathbf{z} - \mathbf{a}\|_1^k \\ &\leq \frac{C_g \|\mathbf{z} - \mathbf{a}\|^\beta}{k!} \left(\sqrt{d} \|\mathbf{z} - \mathbf{a}\| \right)^k = \frac{C_g d^{k/2} \|\mathbf{z} - \mathbf{a}\|^s}{k!}. \end{aligned}$$

□

Lemma 17. [16, Theorem 11.3] Let $\{\mathbf{z}_i\}_{i=n+1}^{2n}$ be i.i.d. sampled from a probability measure μ such that $\text{supp}(\mu) \subseteq [-B, B]^d$ and let $\{y_i\}_{i=n+1}^{2n}$ be sampled from the regression model

$$y = h(\mathbf{z}) + \zeta$$

where $\mathbb{E}[\zeta|\mathbf{z}] = 0$. Suppose $\|h\|_\infty < +\infty$ and $\sup_{\mathbf{z}} \text{var}(\zeta|\mathbf{z}) \leq \bar{\sigma}^2 < \infty$. Let \mathcal{F} be a linear space of functions from \mathbb{R}^d to \mathbb{R} , and \hat{g} be the estimator given by

$$\hat{h} = T_{\|h\|_\infty} \tilde{h} \quad \text{where} \quad \tilde{h} = \arg \min_{p \in \mathcal{F}} \frac{1}{n} \sum_{i=1}^n |p(\mathbf{z}_i) - y_i|^2.$$

Then

$$\begin{aligned} &\mathbb{E} \int |\hat{h}(\mathbf{z}) - h(\mathbf{z})|^2 \mu(d\mathbf{z}) \\ &\leq c \cdot \max(\bar{\sigma}^2, \|h\|_\infty^2) \frac{\dim(\mathcal{F}) \log n}{n} + 8 \inf_{p \in \mathcal{F}} \int |p(\mathbf{z}) - h(\mathbf{z})|^2 \mu(d\mathbf{z}). \end{aligned} \quad (\text{S.7})$$

for some universal constant c .

In (S.7), the mean squared error is decomposed into two terms: the first term captures the variance and the second term estimates the bias. We consider piecewise polynomial approximation with order no more than k such that $\mathcal{F} = \mathcal{F}_k$.

Proof of Lemma 8. In order to apply Lemma 17, we express the regression model in (10) as

$$y_i = \underbrace{g(\mathbf{z}_i) + \eta(\mathbf{z}_i)}_{h(\mathbf{z}_i)} + \underbrace{\tilde{\xi}_i - \eta(\mathbf{z}_i)}_{\zeta_i}$$

with η defined in (12). The function h is bounded: $\|h\|_\infty \leq \|g\|_\infty + \|\eta\|_\infty \leq M + L_g B \|\hat{\Phi} - \Phi\|$. The noise satisfies $\mathbb{E}[\zeta|\mathbf{z}] = 0$ and

$$\begin{aligned} \sup_{\mathbf{z}=\hat{\Phi}^T \mathbf{x}} \text{var}(\zeta|\mathbf{z}) &= \sup_{\mathbf{z}=\hat{\Phi}^T \mathbf{x}} \text{var}\left(\xi + g(\Phi^T \mathbf{x}) - g(\hat{\Phi}^T \mathbf{x}) - \mathbb{E}[g(\Phi^T \mathbf{x}) - g(\hat{\Phi}^T \mathbf{x})|\hat{\Phi}^T \mathbf{x}]\right) \\ &= \sup_{\mathbf{z}=\hat{\Phi}^T \mathbf{x}} \text{var}(\xi) + \text{var}[g(\Phi^T \mathbf{x}) - g(\hat{\Phi}^T \mathbf{x})|\hat{\Phi}^T \mathbf{x} = \mathbf{z}] \\ &\leq \sigma^2 + L_g^2 B^2 \|\hat{\Phi} - \Phi\|^2 = \sigma^2 + b_{\text{bias}}^2, \end{aligned}$$

where b_{bias}^2 is defined in (13). We apply Lemma 17 with $\mathcal{F} = \mathcal{F}_k$, and then

$$\begin{aligned} &\mathbb{E} \int |\hat{g}(\mathbf{z}) - g(\mathbf{z}) - \eta(\mathbf{z})|^2 \mu(d\mathbf{z}) \\ &\leq c \cdot \max(\sigma^2 + b_{\text{bias}}^2, 2M^2 + 2b_{\text{bias}}^2) \frac{\dim(\mathcal{F}_k) \log n}{n} + 8 \inf_{p \in \mathcal{F}_k} \int |p(\mathbf{z}) - g(\mathbf{z}) - \eta(\mathbf{z})|^2 \mu(d\mathbf{z}). \end{aligned}$$

for some universal c . Here $\dim(\mathcal{F}_k)$ is the dimension of \mathcal{F}_k and hence $\dim(\mathcal{F}_k) = \binom{d+k}{d} K^d$. Let g_k be the piecewise Taylor polynomial of g with degree no more than $k = \lfloor s+1 \rfloor - 1$ on the partition of $[-B, B]^d$ into K^d cubes, where the Taylor expansion is at the center of each cube. The second term can be estimated from Lemma 16 as

$$\begin{aligned} \inf_{p \in \mathcal{F}_k} \int |p(\mathbf{z}) - g(\mathbf{z}) - \eta(\mathbf{z})|^2 \mu(d\mathbf{z}) &\leq \sup_{\mathbf{z}} |g_k(\mathbf{z}) - g(\mathbf{z}) - \eta(\mathbf{z})|^2 \\ &\leq 2 \left(\frac{C_g d^{k/2}}{k!} \left(\frac{B d^{1/2}}{K} \right)^s \right)^2 + 2\|\eta\|_\infty^2 \leq \frac{2C_g^2 B^{2s} d^{s+k}}{(k!)^2 K^{2s}} + 2b_{\text{bias}}^2. \end{aligned}$$

Therefore

$$\begin{aligned} &\mathbb{E} \int |\hat{g}(\mathbf{z}) - g(\mathbf{z}) - \eta(\mathbf{z})|^2 \mu(d\mathbf{z}) \\ &\leq c \cdot \max(\sigma^2 + b_{\text{bias}}^2, 2M^2 + 2b_{\text{bias}}^2) \frac{\binom{d+k}{d} K^d \log n}{n} + \frac{2C_g^2 B^{2s} d^{s+k}}{(k!)^2 K^{2s}} + 2b_{\text{bias}}^2. \end{aligned}$$

We have

$$\begin{aligned} &\mathbb{E} \int |\hat{g}(\mathbf{z}) - g(\mathbf{z})|^2 \mu(d\mathbf{z}) = \mathbb{E} \int |\hat{g}(\mathbf{z}) - g(\mathbf{z}) - \eta(\mathbf{z}) + \eta(\mathbf{z})|^2 \mu(d\mathbf{z}) \\ &\leq \mathbb{E} \left(2 \int |\hat{g}(\mathbf{z}) - g(\mathbf{z}) - \eta(\mathbf{z})|^2 \mu(d\mathbf{z}) + 2 \int |\eta(\mathbf{z})|^2 \mu(d\mathbf{z}) \right) \\ &\leq 2c \cdot \max(\sigma^2 + b_{\text{bias}}^2, 2M^2 + 2b_{\text{bias}}^2) \frac{\binom{d+k}{d} K^d \log n}{n} + \frac{4C_g^2 B^{2s} d^{s+k}}{(k!)^2 K^{2s}} + 6b_{\text{bias}}^2. \end{aligned}$$

□

G Proof of (19)

Proof of (19). We have

$$\begin{aligned}\|\widehat{\Phi} - \Phi\|^2 &\leq \sum_{i=1}^d \|\widehat{\phi}_i - \phi_i\|^2 \\ &= \sum_{i=1}^d \widehat{\phi}_i^T \widehat{\phi}_i + \phi_i^T \phi_i - \widehat{\phi}_i^T \phi_i - \phi_i^T \widehat{\phi}_i \\ &= \sum_{i=1}^d 2 - 2 \cos(\theta_i) \leq \sum_{i=1}^d 2(1 - \cos^2(\theta_i)) \\ &= \sum_{i=1}^d 2 \sin^2(\theta_i) \leq 2d \sin^2(\theta_1) \\ &= 2d \|\text{Proj}_{\widehat{\Phi}} - \text{Proj}_{\Phi}\|^2.\end{aligned}$$

The last equality comes from [35, Theorem 5.5].

□